International Journal of Non-Linear Mechanics 118 (2020) 103288

Contents lists available at ScienceDirect

International Journal of Non-Linear Mechanics

journal homepage: www.elsevier.com/locate/nlm

Magnetorheological Fluids: Qualitative comparison between a mixture model in the Extended Irreversible Thermodynamics framework and an Herschel–Bulkley experimental elastoviscoplastic model

Mario Versaci [a,*], Annunziata Palumbo [b]

[a] DICEAM Department, "Mediterranea" University, Via Graziella Feo di Vito, I-89122 Reggio Calabria, Italy
[b] MIFT Department, Messina University, Via F. Stagno d'Alcontres, I-98166 Messina, Italy

ARTICLE INFO

Keywords:
MR fluids
Mixture models
Extended Irreversible Thermodynamics theory
Generalized standard materials
Elastoviscoplasticity

ABSTRACT

A well-known mixture approach treats magnetorheological materials as mixtures composed of a fluid continuum and an equivalent solid continuum. In the framework of extended irreversible thermodynamics, this obtains a complete physical-mathematical model characterized by interesting evolutionary constitutive equations which, in the pre-yield region, show the co-presence of elastic, viscoelastic, and viscoplastic behaviors. Due to its high computational complexity, it is necessary to find a qualitatively corresponding model that, under the same conditions, provides easy-to-implement evolutionary constitutive equations. In this paper, the authors verify the correspondence of the simple shear flow and thinning behavior of the Herschel–Bulkley plastic component (predominant in the pre-yielding region) from a known experimental model with a reduced computation load with elastoviscoplastic generalization under the framework of generalized standard materials.

1. Introduction to the problem

Magnetorheological Fluids (MR Fluids), consisting of polarizable fine particles of suspended ferromagnetic material in mineral oil or aqueous solution, are controllable fluids whose rheological characteristics change abruptly and reversibly depending on the impressed magnetic field $\mathbf{H}$ [1–4]. In the absence of $\mathbf{H}$, these fluids behave as liquids with a viscosity comparable to that of mineral oils. Applying $\mathbf{H}$, a magnetic moment is induced on the particles which forces the dipoles to join in chains, parallel to the lines of force of $\mathbf{H}$, to form columns that reduce fluid mobility and increase viscosity [5,6]. To overcome the friction that arises from the mutual movement of the columns, we need to overcome a threshold of shear stress, τ_0 (yield stress), depending on the impressed $\mathbf{H}$ [7]. Varying $|\mathbf{H}|$, τ_0 will vary, controlling the fluid's ability to transmit forces [8,9]. To determine the intended use of a device containing MR fluid, the pre-yielding phase assumes particular importance. From a theoretical point of view, in recent decades, scientific research has produced sophisticated and complete but computationally prohibitive models [10–14]. Among them, Chen & Yeh's model stands out[1] in the framework of Extended Irreversible Thermodynamics (EIT) in the sense of Jou et al. [15] considered MR material to be a mixture of a fluid continuum and an equivalent solid continuum and obtained evolutionary constitutive equations. This model, around the yield, explicitly highlights the co-presence of elastic, viscoelastic, and viscoplastic behaviors [16]. In parallel, researchers have worked hard on the experimental modeling of industrial interest to formulate models with low computational complexity that are respectful of the different macroscopic behaviors of MR fluids when the shear rate in the rheometer direction, $\dot{\gamma}$, is variable[2] [17–19]. These models fix the electrical current I (scalar value) and fit experimental measurements of shear stress in the rheometer direction, τ,[3] depending on both $\dot{\gamma}$ and temperature θ, producing the so-called flow curves, $\tau(\dot{\gamma},\theta)$, which are significantly related to the magnetorheological behavior of the fluid. Usually, $\tau(\dot{\gamma},\theta)$ provides evidence of quasi-linear behavior within a given shear rate value, indicated by $\dot{\gamma}^*$, beyond which the non-linearity is markedly evident. So, for $\dot{\gamma} < \dot{\gamma}^*$, Newtonian models are used, while for $\dot{\gamma} > \dot{\gamma}^*$, the modeling takes place through plastic formulations. Then, we consider $\tau(\dot{\gamma},\theta)$ as a weighted sum of two models; the first one is Newtonian, while the second one is non-linear so that for $\dot{\gamma} > \dot{\gamma}^*$, plasticity prevails. For example, in the D.S. Resiga model [20],[4] the plastic contribution is modeled by means of a Herschel–Bulkley approach. It therefore appears necessary to find a link between theoretical completeness and experimental pragmatism in order to obtain, at least

* Corresponding author.
E-mail addresses: mario.versaci@unirc.it (M. Versaci), apalumbo@unime.it (A. Palumbo).

[1] Elaborated by K.C. Chen, National Chi-Nan University (Taiwan) & C.S. Yeh, National Taiwan University (Taiwan).
[2] $\dot{\gamma}$ is a tensor that becomes a scalar in the rheometer direction.
[3] τ is a tensor, but, in the rhemometer direction, it can be considered scalar.
[4] Elaborated by D.S. Resiga, University of Timisoara (Romania).

https://doi.org/10.1016/j.ijnonlinmec.2019.103288
Received 22 July 2019; Received in revised form 2 September 2019; Accepted 25 September 2019
Available online 26 September 2019
0020-7462/

in principle, translations with a low computational load of theoretical models that are difficult to implement. In particular, in this work, we provide evidence of the qualitative link between the theoretical mixture model elaborated by Chen & Yeh and the experimental D.S. Resiga model in simple shear flow with thinning behavior. However, it is observed that, in the pre-yield region, the D.S. Resiga model is identified only by the power-law Herschel–Bulkley plastic component, which is not evolutionary and, moreover, does not explicitly manifest the co-presence of elastic, viscoelastic, and viscoplastic behaviors as evidenced, under the same conditions, by the Chen & Yeh model. Hence, the need to generalize the Herschel–Bulkley plastic component of the D.S. Resiga model to achieve its elastoviscoplastic formulation (EVP) suitable for qualitative comparison with the Chen & Yeh model. This was possible by using the framework of the Generalized Standard Materials (GSMs) according to the Halphen & Nguyen approach [21]. The correspondence between the two models was then formalized by means of a set of propositions with qualitative statements.

The paper is organized as follows: Section 2 shows the main results of the Chen & Yeh theoretical model, which was to formulate, in the framework of the EIT, evolutionary constitutive equations that are valid in the pre-yield region . Section 3, describes, in detail, the structure of the D.S. Resiga experimental model, specifying its particularization in the pre-yield region. Section 4 reports, in the framework of the GSMs, the $3D$ dimensionless EVP generalization of the Herschel–Bulkley plastic component of the D.S. Resiga model obtaining, even in this case, evolutionary constitutive equations that are useful for the comparison with the theoretical model. Section 5 highlights the importance, if the comparison is feasible, for the theoretical model to be formulated in the framework of the EIT and for the experimental model to be structured within the GSMs. The details of the qualitative correspondence between the two approaches are provided . In particular, two Remarks justify the operational choices related to the plasticity criteria function, and subsequently, five Propositions with qualitative statements detail the correspondence between the theoretical model and the experimental one under the chosen operating conditions. Since the adopted approach implies a simplification of the Herschel–Bulkley EVP generalization, Section 6 reports some numerical tests which, by comparison with two benchmarks that are well-known in literature, show that the loss of information contained in this simplification can be considered negligible. Finally, some summary considerations and future perspectives conclude the work. To facilitate reading, Tables 1 and 2 provide lists of the symbols used and the acronyms exploited.

2. Chen & Yeh mixture model: An overview

2.1. Positions and velocities

MR materials, under the effect of external $|\mathbf{H}|$ are endowed with a body-centered tetragonal structure with lower energy with respect to other structures [16] . Chen & Yeh considered MR material to be a mixture composed by a fluid continuum, F, and an equivalent solid continuum, S, that simultaneously occupy the same region of space. S and F continua are indicated by the material points ξ^F and ξ^S, respectively. In addition, the material points are identified by their position vectors ξ^F_α and ξ^S_α. For each instant t, positions are assigned to material points $x^F_i = x^F_i(\xi^F_\alpha, t)$ and $x^S_i = x^S_i(\xi^S_\alpha, t)$. According the hypotheses made above, $x_i = x^F_i = x^S_i$, from which the velocity vectors are determined to be

$$v^F_i = \frac{d_F x^F_i}{dt}; \quad v^S_i = \frac{d_S x^S_i}{dt} \tag{1}$$

with

$$\frac{d_S}{dt} = \frac{d}{dt} + (v^S_k - v_k)\frac{\partial}{\partial x_k} = \frac{d}{dt} - \left(\frac{\rho^F v^R_k}{\rho}\right)\frac{\partial}{\partial x_k} \tag{2}$$

$$\frac{d_F}{dt} = \frac{d}{dt} + (v^F_k - v_k)\frac{\partial}{\partial x_k} = \frac{d}{dt} + \left(\frac{\rho^S v^R_k}{\rho}\right)\frac{\partial}{\partial x_k} \tag{3}$$

material derivatives for fixed ξ^F_α and ξ^S_α, respectively, and the usual summation convention for the double contraction of indices is used. ρ^F, ρ^S and ρ indicate the densities of the fluid, solid, and the whole mixture, so that $\rho = \rho^F + \rho^S$, the mean velocity of the mixture, at (x_i, t), is written as $v_i = \dot{x}_i = \frac{dx_i}{dt} = \frac{1}{\rho}(\rho^F v^F_i + \rho^S v^S_i)$, while the diffusion velocities are defined as $\overline{v_i}^F = v^F_i - v_i$; $\overline{v_i}^S = v^S_i - v_i$, and the relative velocity vector of the fluid to the solid is given by $v^R_i = v^F_i - v^S_i$. Since the solid continuum in [16] is considered to be a set of magnetizable particles, and exploiting the concept of "intermediate state" proposed by Lee [22,23] to decompose the solid continuum deformation, we denote the position of the material point in the solid continuum in the reference, released intermediate, and final positions as ξ^S_α, X^S_I, and x^S_i, respectively. Physically, intermediate states occur when the current stress state is annulled and the hyperelastic response of the material is characterized. In addition, to take into account the displacements between each of the two different states, three vectors, $\mathbf{u}^S$, $\mathbf{u}^{SP}$, and $\mathbf{u}^{SE}$ (with $\mathbf{u}^{SP} + \mathbf{u}^{SE} = \mathbf{u}^S$, $\xi^S + \mathbf{u}^{SP} = X^S$ and $\xi^S + \mathbf{u}^S = x$) are introduced. Specifically,

$$u^S_i(x_i, t) = x_i - \delta_{i\alpha}\xi^S_\alpha \tag{4}$$

$$u^S_i = u^{SE}_i + \delta_{iK}u^{SP}_K \tag{5}$$

$$u^{SE}_i = x_i - \delta_{iK}X^S_K. \tag{6}$$

The intermediate state, obviously, is an artificial state that is exploited to separate plastic and elastic deformation.

2.2. Velocity gradient tensor and elastic strain tensors

If we indicate the elastic and plastic components of the velocity gradient tensor L^S_{ij} by L^{SE}_{ij} and L^{SP}_{ij}, respectively, the following relation yields

$$L^S_{ij} = \frac{\partial v^S_i}{\partial x_j} = L^{SE}_{ij} + F^{SE}_{iI}L^{SP}_{IJ}(F^{SE}_{jJ})^{-1} = L^{SE}_{ij} + L^{SP}_{ij} \tag{7}$$

where $L^{SE}_{ij} = \frac{d_S}{dt}\left(\frac{\partial x_i}{\partial X^S_I}\right)\frac{\partial X^S_I}{\partial x_j}$, $L^{SP}_{IJ} = \frac{d_S}{dt}\left(\frac{\partial X^S_I}{\partial \xi^S_\alpha}\right)\frac{\partial \xi^S_\alpha}{\partial X^S_J}$ and $F^{SE}_{iI} = \frac{\partial x_i}{\partial X^S_I}$. Considering (7) again, we decompose L^S_{ij} in its symmetric part, $L^S_{(ij)}$, and its antisymmetric one, $L^S_{[ij]}$:

$$L^S_{(ij)} = D^S_{ij} = D^{SE}_{ij} + F^{SE}_{(iI}L^{SP}_{IJ}(F^{SE}_{j)J})^{-1} = D^{SE}_{ij} + D^{SP}_{ij} \tag{8}$$

$$L^S_{[ij]} = \Omega^S_{ij} = \Omega^{SE}_{ij} + F^{SE}_{[iI}L^{SP}_{IJ}(F^{SE}_{j]J})^{-1} = \Omega^{SE}_{ij} + \Omega^{SP}_{ij} \tag{9}$$

from which it is clear that $L^S_{(ij)}$ takes both elongations and distortions (D^{SE}_{ij}, D^{SP}_{ij}) into account, while $L^S_{[ij]}$ takes rotations (Ω^{SE}_{ij}, Ω^{SP}_{ij}) into account.

The Lagrangian elastic strain tensor,

$$E^{SE}_{IJ} = \frac{1}{2}\left(\frac{\partial x_i}{\partial X^S_I}\frac{\partial x_i}{\partial X^S_J} - \delta_{IJ}\right), \tag{10}$$

and Eulerian elastic strain tensor,

$$e^{SE}_{ij} = \frac{1}{2}\left(\delta_{ij} - \frac{\partial X^S_K}{\partial x_i}\frac{\partial X^S_K}{\partial x_j}\right) = E^{SE}_{IJ}\frac{\partial X^S_I}{\partial x_i}\frac{\partial X^S_J}{\partial x_j}, \tag{11}$$

can be used as strain measures, from which

$$\frac{d_S}{dt}E^{SE}_{IJ} = D^{SE}_{ij}\frac{\partial x_i}{\partial X^S_I}\frac{\partial x_j}{\partial X^S_J} \tag{12}$$

and

$$\frac{d_S}{dt}e^{SE}_{ij} = D^{SE}_{ij} - e^{SE}_{kj}L^{SE}_{ki} - e^{SE}_{ki}L^{SE}_{kj} \tag{13}$$

where

$$e^{SE}_{ij} = \frac{1}{2}(u^{SE}_{i,j} + u^{SE}_{j,i} - u^{SE}_{k,i}u^{SE}_{k,j}) \tag{14}$$

and $_{,i} \equiv \frac{\partial}{\partial x_i}$ stands for the partial derivatives by coordinates. In particular, (14) represents the link between the elastic deformation and the displacement gradient.

Table 1
List of the exploited symbols.

Symbol	Description
$\mathbf{H}$, $\mathbf{B}$,	magnetic field, magnetic induction,
$\mathbf{E}$, I	electrostatic field and electrical current
$\dot{\gamma}$, τ_0	shear rate in the rheometer direction and yield stress
$\dot{\gamma}^*$	shear rate in the rheometer direction around the transition from Newtonian to plastic behavior
θ, θ_0	temperature and room temperature
ξ^S, ξ^F	positions of the solid and fluid continua
x_i^S, x_i^F	assigned positions to solid and fluid material points
ξ_α^S, X_I^S, x_i^S	reference, intermediate, and final positions of the material points in the solid continuum
v_i^S, v_i^F	velocity vectors of solid and fluid
ρ^S, ρ^F, ρ	densities of the solid, fluid, and mixture
v_i, v_i^R	velocity of the mixture and relative velocity vector
$\overline{v}_i^S$, $\overline{v}_i^F$	diffusion velocities of the solid and fluid
p^F	equilibrium pressure of the fluid
L_{ij}^S	velocity gradient tensor
L_{ij}^{SE}, L_{ij}^{SP}	elastic and plastic components of the velocity gradient tensor
$L_{(ij)}^S$, $L_{[ij]}^S$	symmetric antisymmetric part of L_{ij}^S
Ω_{ij}^S, Ω_{ij}^{SE}, Ω_{ij}^{SP}	vorticity tensor referring to the solid continuum and its elastic and plastic parts
e_{ij}^{SE}, E_{IJ}^{SE}	Eulerian and Lagragian elastic strain tensors
τ_{ij}	stress tensor
τ_{ij}^S, τ_{ij}^F	solid and fluid stress tensors
τ_{ij}^{FS}, τ^{FB}	stress tensors referring to the shear and bulk parts of the fluid
τ_{ij}^{SR}, τ_{ij}^{SD}	reversible and dissipative parts of the solid stress tensor
M_i^S	magnetization
M_i^{SR}, M_i^{SD}	reversible and dissipative parts of the magnetization
e_{ijk}	alternative tensor
ϵ_0, μ_0	permittivity and permeability in a vacuum
P_i	momentum supply to the solid
f_i^S, f_i^F	external body forces of the solid and fluid
U^S, U^F	internal energy densities of the solid and fluid
q_i^S, q_i^F	heat fluxes of the solid and fluid
h^S, h^F	internal heat sources of the solid and fluid
η^S, η^F	entropy densities of the solid and fluid
S_i^S, S_i^F	entropy fluxes of the solid and fluid
S_i, η	entropy flux and entropy density of the mixture
H	Helmotz free energy of the mixture
$\tau^{\alpha\beta}$	characteristic times
μ, μ^S, μ^B	viscosity, shear and bulk viscosities
K, n	consistency parameter and power law index
π_p, π_0	viscosity in the rheometer direction and total viscosity
ζ, T, Σ, Π	relaxation time, characteristic time of the shear flow, characteristic stress of the flow and slowdown parameter
$\mathcal{D}$	potential for dissipation in the SG framework
∂D	sub-differential of a tensor D
V, L	characteristic velocity and length of the flow
ϵ_{ij}, ϵ_{ij}^E, ϵ_{ij}^P	elastic deformation tensor and its elastic and plastic parts
$\lvert\mathrm{E}\rvert$, $\lvert\mathrm{E}^E\rvert$, $\lvert\mathrm{E}^P\rvert$	matrix norm of ϵ_{ij}, ϵ_{ij}^E, ϵ_{ij}^P, respectively
ω	parameter of elasticity
$(\tau_{ij})_d$	deviatoric part of τ_{ij}
$\lvert\mathrm{T}_d\rvert$	matrix norm of $(\tau_{ij})_d$
$\frac{D_a\tau_{ij}}{Dt}$	Gordon–Schowalter derivative
$k_n(s)$	plasticity criteria function
Re, We, Bi	Reynolds, Weissenberg, and Bingham numbers
Θ	frequency

Table 2
List of the exploited acronyms.

Acronym	Description
MR	magnetorheological
EIT	extended irreversible thermodynamics
EVP	elastoviscoplastic
F	fluid fraction
E	elastic component
P	plastic component
FB	bulk part of the fluid
FS	shear part of the fluid
HB	Herschel–Bulkley
N	Newtonian
S	solid fraction
GSM	generalized standard material

2.3. Stress tensors

It is assumed that the fluid stress tensor is a symmetric tensor, $\tau_{ij}^F = \tau_{ji}^F$, while for the stress tensor of the solid continuum, due to the application of the external $\mathbf{H}$, $\tau_{ij}^S \neq \tau_{ji}^S$. Then, the following further decompositions are assumed:

$$\tau_{ij}^F = \tau_{ji}^F = -p^F\delta_{ij} + \tau^{FB}\delta_{ij} + \tau_{ij}^{FS}, \quad \tau_{ii}^{FS} = 0 \tag{15}$$

$$\tau_{ij}^S = \tau_{ij}^{SR} + \tau_{ij}^{SD} = \tau_{(ij)}^{SR} + \tau_{[ij]}^{SR} + \tau_{ij}^{SD}, \quad \tau_{ij}^{SD} = -\tau_{ji}^{SD} \tag{16}$$

in which the superscripts FB and FS refer to the bulk of the fluid and the shear fluid, respectively; SR and SD represent, respectively, the reversible part and dissipative part of the solid continuum (represented by an antisymmetric tensor). Again, in (15), p^F is the equilibrium pressure of the fluid, while τ^{FB} and τ_{ij}^{FS} are the quantities induced in the non-equilibrium state due to the dissipative viscous mechanical forces, and, obviously they vanish at equilibrium. In addition, considering the angular momentum balance, the antisymmetric part of the stress is associated with the magnetization M_i^S, $\tau_{[ij]}^S = -M_{[i}^S B_{j]}^S$, B_j^S being the magnetic induction [16]. Moreover, by decomposing the magnetization into a reversible part, M_i^{SR}, and a dissipative part M_i^{SD}, that is $M_i^S = M_i^{SR} + M_i^{SD}$, it is possible to write

$$\tau_{[ij]}^{SR} = -M_{[i}^{SR} B_{j]}^S; \quad \tau_{[ij]}^{SD} = -M_{[i}^{SD} B_{j]}^S. \tag{17}$$

2.4. Field equations

Since MR fluids are composed of magnetizable particles in mineral oil, in [16] it is postulated that the fluid continuum is the non-magnetizable fraction of the material, while the solid continuum is sensitive to the actions due to the external $\mathbf{H}$. In such a context, Maxwell equations can only be written for the solid continuum:

$$\begin{cases} B_{i,i}^S = 0 \\ \epsilon_0 E_{i,i}^S = 0 \\ e_{ijk}E_{kj}^S + \frac{\partial B_i^S}{\partial t} = 0 \\ \frac{1}{\mu_0} e_{ijk} B_{k,j}^S - \epsilon_0 \frac{\partial E_i^S}{\partial t} = e_{ijk} M_{k,j}^S \end{cases} \tag{18}$$

where e_{ijk} is the alternative tensor, and E_i^S, B_i^S, ϵ_0, and e μ_0 denote the electrostatic field, the magnetic induction, the permittivity, and the permeability in the vacuum, respectively. If there are no chemical reactions, the balanced equations of mass, linear momentum, and energy for the fluid continuum can be written as follows:

$$\begin{cases} \frac{\partial \rho^F}{\partial t} + (\rho^F v_k^F)_{,k} = 0; \quad \rho^F \frac{d_F v_i^F}{dt} = \tau_{ji,j}^F - P_i + \rho^F f_i^F \\ \rho^F \frac{d_F U^F}{dt} = \tau_{ji}^F v_{i,j}^F - q_{i,i}^F + \rho^F h^f + P_i v_i^F \end{cases} \tag{19}$$

while, for the solid continuum, they are

$$\begin{cases} \frac{\partial \rho^S}{\partial t} + (\rho^S v_k^S)_{,k} = 0; \quad \rho^S \frac{d_S v_i^S}{dt} = \tau_{ji,j}^S + B_{j,i}^S M_j^S + P_i + \rho^S f_i^S \\ \rho^S \frac{d_S U^S}{dt} = \tau_{ji}^S v_{i,j}^S - q_{i,i}^S - M_i^S \frac{d_s B_i^S}{dt} + \rho^S h^S - P_i v_i^S \end{cases} \tag{20}$$

where P_i denotes the momentum supply to the solid; f_i^F and f_i^S are the external body forces of the fluid and solid respectively; U^F and U^S represent the internal energy densities of the fluid and the solid respectively; q_i^F and q_i^S are the heat fluxes of the fluid and the solid, respectively; and h^F and h^S denote the internal heat sources of the fluid and solid respectively. By combining (19) with (20), we obtain the following balanced equations:

$$\begin{cases} \rho \frac{dU}{dt} = \tau_{ji}^F v_{i,j}^F + \tau_{ji}^S v_{i,j}^S - q_{i,i} - M_i^S \frac{d_S B_i^S}{dt} + \rho h + P_i(v_i^F - v_i^S) \\ \rho U = \rho^F U^F + \rho^S U^S; \quad \rho h = \rho^F h^F + \rho^S h^S \\ q_i = q_i^F + q_i^S + \rho^F U^F (v_i^F - v_i) + \rho^S U^S (v_i^S - v_i). \end{cases} \tag{21}$$

On the other hand, the local version of the second law of the thermodynamics for both solid and fluid continua can be written as follows:

$$\begin{cases} \rho^F \frac{d_F \eta^F}{dt} + S_{i,i}^F - \rho^F \frac{h^F}{\theta} \geq 0 \\ \rho^S \frac{d_S \eta^S}{dt} + S_{i,i}^S - \rho^S \frac{h^S}{\theta} \geq 0 \end{cases} \tag{22}$$

where both the continua are assumed to be at the same temperature θ, while η^F, η^S, S_i^F, and S_i^S represent the entropy densities of the fluid and the solid and the entropy fluxes of the fluid and solid, respectively. By introducing the entropy density η and the entropy flux S_i of the mixture, both previous equations can be combined to achieve the following system:

$$\begin{cases} \rho\theta \frac{d\eta}{dt} + \theta S_{i,i} - \rho h \geq 0 \\ \rho\eta = \rho^F \eta^F + \rho^S \eta^S \\ S_i = S_i^F + S_i^S + \rho^F \eta^F (v_i^F - v_i) + \rho^S \eta^S (v_i^S - v_i). \end{cases} \tag{23}$$

If, finally, one introduces the Helmotz free energy of the mixture, $H = U - \eta\theta$, Eqs. (21) and (23) can be rearranged as the following inequality:

$$-\rho \frac{dH}{dt} - \rho\eta \frac{d\theta}{dt} + \theta S_{i,i} + \tau_{ji}^F v_{i,j}^F + \tau_{ji}^S v_{i,j}^S - q_{i,i} - M_i^S \frac{d_S B_i^S}{dt} + P_i v_i^R \geq 0. \tag{24}$$

To obtain, on the one hand, a more general thermodynamic theory of MR fluids and, on the other hand, to achieve evolutionary constitutive equations, it is imperative to frame the approach in the framework of the EIT [15] in which the Helmotz free energy depends on both a set of conserved variables, θ, ρ^F, e_{ij}^{SE}, B_i^S, and some fluxes, q_i, M_i^{SD}, v_i^R, τ_{ij}^{FS}, τ^{FB}:

$$H = H(\underbrace{\theta, \rho^F, e_{ij}^{SE}, B_i^S}_{conserved\ variables}; \underbrace{q_i, M_i^{SD}, v_i^R, \tau_{ij}^{FS}, \tau^{FB}}_{fluxes}). \tag{25}$$

By exploiting the material derivatives by virtue of (2) and (3), we have

$$\frac{dH}{dt} = \frac{\partial H}{\partial \theta}\frac{d\theta}{dt} + \frac{\partial H}{\partial \rho^F}\frac{d_F\rho^F}{dt} + \frac{\partial H}{\partial e_{ij}^{SE}}\frac{d_S e_{ij}^{SE}}{dt} + \frac{\partial H}{\partial B_i^S}\frac{d_S B_i^S}{dt} + \frac{\partial H}{\partial q_i}\frac{dq_i}{dt} + \tag{26}$$

$$+ \frac{\partial H}{\partial M_i^{SD}}\frac{d_S M_i^{SD}}{dt} + \frac{\partial H}{\partial v_i^R}\frac{dv_i^R}{dt} + \frac{\partial H}{\partial \tau_{ij}^{FS}}\frac{d_F \tau_{ij}^{FS}}{dt} + \frac{\partial H}{\partial \tau^{FB}}\frac{d_F \tau^{FB}}{dt} + \frac{1}{\rho} v_k^R A_k$$

with

$$A_k = -\rho^S \frac{\partial H}{\partial \rho^F}\rho_{,k}^F + \rho^F \frac{\partial H}{\partial e_{ij}^{SE}} e_{ij,k}^{SE} + \rho^F \frac{\partial H}{\partial B_i^S} B_{i,k}^S + \rho^F \frac{\partial H}{\partial M_i^{SD}} - \rho^S \frac{\partial H}{\partial \tau_{ij}^{FS}} \tau_{ij,k}^{FS} - \rho^S \frac{\partial H}{\partial \tau^{FB}} \tau_{,k}^{FB}. \tag{27}$$

As with classical thermodynamics (reversible), the generalized entropy density, η, the equilibrium pressure of the fluid, p^F, the reversible stress of the solid, τ_{ij}^{SR}, and the reversible part of magnetization, M_i^{SR},

are defined as follows:

$$\eta = -\frac{\partial H}{\partial \theta}, \quad p^F = \rho\rho^F \frac{\partial H}{\partial \rho^F}, \quad \tau_{ij}^{SR} = \rho\Big(\frac{\partial H}{\partial e_{ij}^{SE}} - 2\frac{\partial H}{\partial e_{ik}^{SE}} e_{kj}^{SE}\Big),$$
$$M_i^{SR} = -\rho\frac{\partial H}{\partial B_i^S}. \tag{28}$$

Note that from (17) and exploiting the definitions of the reversible parts of the solid and the magnetization in (28), it makes sense to write

$$\tau_{(ij)}^{SR} = \rho\Big(\frac{\partial H}{\partial e_{ij}^{SE}} - \frac{\partial H}{\partial e_{ik}^{SE}} e_{kj}^{SE} - \frac{\partial H}{\partial e_{jk}^{SE}} e_{ki}^{SE}\Big) \tag{29}$$

$$\tau_{[ij]}^{SR} = -\rho\Big(\frac{\partial H}{\partial e_{ik}^{SE}} e_{kj}^{SE} - \frac{\partial H}{\partial e_{jk}^{SE}} e_{ki}^{SE}\Big) = -M_{[i}^{SR} B_{j]}^S = \rho\frac{\partial H}{\partial B_{[i}^S} B_{j]}^S. \tag{30}$$

Obviously, Eq. (30) shows that the elastic deformation for the solid continuum is directly proportional to the magnetization induced by the external $|\mathbf{H}|$. D_{ij}^F indicates the tensor that takes the elongations of the fluid into account, and the decomposition of the stress tensor permits the stress powers to be written as

$$\tau_{ji}^F v_{i,j}^F = -p^F v_{i,i}^F + \tau^{FB} v_{i,i}^F + \tau_{ij}^{FS} D_{ij}^F \tag{31}$$

$$\tau_{ji}^S v_{i,j}^S = \tau_{(ji)}^{SR} D_{ij}^{SE} + \tau_{(ji)}^{SR} D_{ij}^{SP} - M_{[j}^{SD} B_{i]}^S \Omega_{ij}^S - M_{[j}^{SR} B_{i]}^S \Omega_{ij}^S. \tag{32}$$

Moreover, in the linear approximation, the derivatives of free energy with respect to the fluxes can be expressed by the following equations:

$$\begin{cases} \rho\frac{\partial F}{\partial q_i} = \lambda_{11} q_i + \lambda_{12} M_i^{SD} + \lambda_{13} v_i^R \\ \rho\frac{\partial F}{\partial M_i^{SD}} = \lambda_{21} q_i + \lambda_{22} M_i^{SD} + \lambda_{23} v_i^R \\ \rho\frac{\partial F}{\partial v_i^R} = \lambda_{31} q_i + \lambda_{32} M_i^{SD} + \lambda_{33} v_i^R \\ \rho\frac{\partial F}{\partial \tau_{ij}^{FS}} = \lambda_4 \tau_{ij}^{FS} \\ \rho\frac{\partial F}{\partial \tau^{FB}} = \lambda_5 \tau^{FB} \end{cases} \tag{33}$$

where $\lambda_{ij} = \lambda_{ji}$ are scalars depending on the variables conserved by means of θ, ρ^F and both the algebraic invariants of e_{ij}^{SE} and B_i^S. It is worth highlighting that $\lambda_{ij} = \lambda_{ji}$ is a consequence of the equality of the mixed derivatives of the free energy after applying Schwarz's theorem, and λ_4 and λ_5 do not explicitly depend on B_i^S. Under the assumption of linear approximation, λ_{ij} functionally depends on θ, ρ^F and e_{ii}^{SE}, i.e., the conserved variables are explicit in Eq. (33). So, taking into account (26), (28), (31), (32), and (33), inequality (24) can be rewritten as follows:

$$\tau_{ji}^{SR} L_{ij}^{SP} + q_i X_i^q + M_i^{SD} X_i^M + v_i^R X_i^v + \tau_{ij}^{FS} X_{ij}^{FS} + \tau^{FB} X^{FB} \geq 0 \tag{34}$$

where X_i^q, X_i^M, X_i^v, X_{ij}^{FS}, and X^{FB} are the thermodynamic forces defined by

$$\begin{cases} X_i^q = -\frac{\theta_{,i}}{\theta} - \lambda_{11}\frac{dq_i}{dt} - \lambda_{21}\frac{d_S M_i^{SD}}{dt} - \lambda_{31}\frac{dv_i^R}{dt} \\ X_i^M = -\frac{d_S B_i^S}{dt} - B_j^S \Omega_{ji}^S - \lambda_{12}\frac{dq_i}{dt} - \lambda_{22}\frac{d_S M_i^{SD}}{dt} - \lambda_{32}\frac{dv_i^R}{dt} \\ X_i^v = P_i - A_i - \lambda_{13}\frac{dq_i}{dt} - \lambda_{23}\frac{d_S M_i^{SD}}{dt} - \lambda_{33}\frac{dv_i^R}{dt} \\ X_{ij}^{FS} = D_{ij}^F - \lambda_4\frac{d_F \tau_{ij}^{FS}}{dt} \\ X^{FB} = v_{i,i}^F - \lambda_5\frac{d_F \tau^{FB}}{dt}. \end{cases} \tag{35}$$

Inequality (34) shows that the motion of the solid continuum contributes to dissipation by means of the term $\tau_{ji} L_{ij}^{SP}$, which results from the elastic stress multiplied by the plastic part of the velocity gradient of the solid; this is compatible with the yield condition when a shear force is applied in excess. τ_{ij}^{SR}, obviously, corresponds to the yield stress and the third condition in (28), and it is relevant for the deformation of the solid continuum (magnetic-induced). The terms $q_i X_i^q$ and $M_i^{SD} X_i^M$ represent the dissipation due to heat conduction and the irreversible magnetization, respectively. The quantity of $v_i^R X_i^v$, a term typically associated with the mixture approach, describes the diffusive dissipation. The last two terms, $\tau^{FB} X^{FB}$ and $\tau_{ij}^{FS} X_{ij}^{FS}$, represent the dissipation from the motion of the viscous fluid continuum. Then, τ^{FB} and τ_{ij}^{FS} represent the mechanical stresses related to FB and FS, respectively, generating the motion of the viscous fluid. τ^{FB} does not need the subscripts $_{ij}$, since is related to the bulk of fluid, while τ_{ij}^{FS}, being related to the shear condition, needs the subscripts $_{ij}$. The main advantage of the mixture approach is in the computation of the diffusive dissipation which is included in the dissipation inequality and is useful for evaluating the evolution of the magnetized particles.

2.5. Evolutionary constitutive equations

To form evolutionary constitutive equations, it is necessary to determine the link between the generalized fluxes and generalized forces. This link, according the Chen & Yeh model [16], is linear:

$$\begin{cases} q_i = \mu^{qq} X_i^q + \mu^{qM} X_i^M + \mu^{qv} X_i^v \\ M_i^{SD} = \mu^{Mq} X_i^q + \mu^{MM} X_i^M + \mu^{Mv} X_i^v \\ v_i^R = \mu^{vq} X_i^q + \mu^{vM} X_i^M + \mu^{vv} X_i^v \\ \tau^{FB} = \mu^B X^{FB} \\ \tau_{ij}^{FS} = \mu^S X_{ij}^{FS}. \end{cases} \tag{36}$$

Finally, by combining (36) with (35), we obtain the following evolution problem:

$$\begin{cases} \tau^{qq}\frac{dq_i}{dt} + \tau^{qM}\frac{d_S M_i^{SD}}{dt} + \tau^{qv}\frac{dv_i^R}{dt} + q_i = -\frac{1}{\theta}\mu^{qq}\theta_{,i} - \mu^{qM}\hat{D}^S B_i^S + \mu^{qv}\overline{P}_i \\ \tau^{Mq}\frac{dq_i}{dt} + \tau^{MM}\frac{d_S M_i^{SD}}{dt} + \tau^{Mv}\frac{dv_i^R}{dt} + M_i^{SD} = -\frac{1}{\theta}\mu^{Mq}\theta_{,i} \\ \quad -\mu^{MM}\hat{D}^S B_i^S + \mu^{Mv}\overline{P}_i \\ \tau^{vq}\frac{dq_i}{dt} + \tau^{vM}\frac{d_S M_i^{SD}}{dt} + \tau^{vv}\frac{dv_i^R}{dt} + v_i^R = -\frac{1}{\theta}\mu^{vq}\theta_{,i} - \mu^{vM}\hat{D}^S B_i^S + \mu^{vv}\overline{P}_i \\ \lambda_4\mu^S\frac{d_F \tau_{ij}^{FS}}{dt} + \tau_{ij}^{FS} = \mu^S D_{ij}^F \\ \lambda_5\mu^B\frac{d_F \tau^{FB}}{dt} + \tau^{FB} = \mu^B v_{i,i}^F \end{cases} \tag{37}$$

in which $\hat{D}^S B_i^S = \frac{d_S B_i^S}{dt} + B_j^S \Omega_{ji}^S$ and $\overline{P}_i = P_i - A_i$, while $\tau^{\alpha\beta}$, $\alpha, and \beta = q, M, v$ are characteristic times. In addition, from the two last equations in (36), it is clear that both μ^B and μ^S represent viscosities (for further details, see [16]).

2.6. The mixture model in the pre-yield region and the evolutionary constitutive equations

In the pre-yield region, the deformation of the fluid continuum and the solid continuum are so small that it is possible to assume that

$$D_{ij}^{SP} = 0; \qquad v_i^F = v_i^S = v_i. \tag{38}$$

Then, inequality (34) can be reduced, despite the effects of heat and irreversible magnetization, to the following inequality:

$$\tau_{ji}^{FS} X_{ij}^{FS} + \tau^{FB} X^{FB} \geq 0 \tag{39}$$

in which

$$\begin{cases} X_{ij}^{FS} = D_{ij}^F - \lambda_4\frac{d_F \tau_{ij}^{FS}}{dt} \\ X^{FB} = v_{i,i}^F - \lambda_5\frac{d_F \tau^{FB}}{dt} \end{cases} \tag{40}$$

implying that MR materials, in the pre-yield region, behave as viscous fluid or viscoelastic bodies, dissipating energy due to their viscosity. However, in the post-yield region, condition (38) cannot take place, and inequality (34) characterizes the mechanisms of energy dissipation. This indicates that MR materials behave as viscoplastic fluids in

the post-yield region. From inequality (39) and taking into account Eq. (40), we can write

$$-\tau_{ij}^{FS}\lambda_4\frac{d_F\tau_{ij}^{FS}}{dt}-\tau^{FB}\lambda_5\frac{d_F\tau^{FB}}{dt}+\tau_{ij}^{FS}D_{ij}^{F}+\tau^{FB}v_{i,i}^{F}\geq 0. \tag{41}$$

In addition, the evolution model (37) can be reduced to the following equations:

$$\begin{cases}\lambda_4\mu^S\frac{d_F\tau_{ij}^{FS}}{dt}+\tau_{ij}^{FS}=\mu^S D_{ij}^{F}\\ \lambda_5\mu^B\frac{d_F\tau^{FB}}{dt}+\tau^{FB}=\mu^B v_{i,i}^{F}.\end{cases} \tag{42}$$

In the following section, inequality (41) and Eq. (42) are exploited in a comparison with the experimental model.

The following remark justifies the use of the EIT framework for the mixture approach.

Remark 2.1. The mixture model proposed by Chen & Yeh in [16] for the pre-yield region, has as its hinge, the system of evolutionary differential equations (42). This formulation makes sense in the EIT framework where the Helmotz free energy, H, depends on (25). If, instead, the approach was framed under classical thermodynamics, the functional dependence of H would be

$$H=H(\underbrace{\theta,\rho^F,e_{ij}^{SE},B_i^S}_{\text{conserved variables}};\underbrace{\quad}_{\text{no fluxes}}) \tag{43}$$

which would produce constitutive relations instead of evolutionary constitutive equations for the dissipative fluxes.

Remark 2.2. As we operate in the pre-yield region, $v_i^F=v_i^S=v_i$, from both (2) and (3), we can write

$$\frac{d_S}{dt}=\frac{d}{dt};\quad \frac{d_F}{dt}=\frac{d}{dt} \tag{44}$$

so that system (42) becomes

$$\begin{cases}\lambda_4\mu^S\frac{d\tau_{ij}^{FS}}{dt}+\tau_{ij}^{FS}=\mu^S D_{ij}^{F}\\ \lambda_5\mu^B\frac{d\tau^{FB}}{dt}+\tau^{FB}=\mu^B v_{i,i}^{F}.\end{cases} \tag{45}$$

Then, for $i=j=1$ and $i=j=2$, system (45) can be written in the following form:

$$\begin{cases}\lambda_4\mu^S\frac{d\tau_{11}^{FS}}{dt}=-\tau_{11}^{FS}+\mu^S D_{11}^{F}\\ \lambda_4\mu^S\frac{d\tau_{22}^{FS}}{dt}=-\tau_{22}^{FS}+\mu^S D_{22}^{F}\\ \lambda_5\mu^B\frac{d\tau^{FB}}{dt}=-\tau^{FB}+\mu^B v_{1,1}^{F}+\mu^B v_{2,2}^{F}.\end{cases} \tag{46}$$

It is worth nothing the fact that in (46), both μ^S and μ^B physically represent viscosities.

3. D.S. Resiga experimental model

3.1. Structure of the model

Experimental investigations have revealed that MR materials behave as quasi-Newtonian fluids with low shear rates in the rheometer direction, $\dot\gamma$, while, for high shear rates, their behavior can be assumed to be plastic [7,21]. The D.S. Resiga model, to grasp both aspects, weights the Newtonian behavior $\tau_N(\dot\gamma)=\mu\dot\gamma$ with the plastic behavior according to the Herschel–Bulkley formulation, $\tau_{HB}(\dot\gamma)=\tau_0+K\left(\frac{\dot\gamma}{\dot\gamma^*}\right)^{1-n}$ (K a consistency parameter) to obtain, by varying the temperature θ, the following power-law model [20]:

$$\tau(\dot\gamma,\theta)=\left\{\tau_N(\dot\gamma)W_1\left(\frac{\dot\gamma}{\dot\gamma^*}\right)+\tau_{HB}(\dot\gamma)W_2\left(\frac{\dot\gamma}{\dot\gamma^*}\right)\right\}_{\theta_0}e^{\frac{E_a}{R}\left(\frac{1}{\theta}-\frac{1}{\theta_0}\right)}= \tag{47}$$

$$=\left\{\mu\dot\gamma W_1\left(\frac{\dot\gamma}{\dot\gamma^*}\right)+\left[\tau_0+K\left(\frac{\dot\gamma}{\dot\gamma^*}\right)^{1-n}\right]W_2\left(\frac{\dot\gamma}{\dot\gamma^*}\right)\right\}_{\theta_0}e^{\frac{E_a}{R}\left(\frac{1}{\theta}-\frac{1}{\theta_0}\right)}$$

in which

1. μ and τ_0 represent the viscosity and the yield stress, respectively [7,20,21];
2. For the fluids with shear-thinning behavior, $n<1$;
3. θ_0 is the room temperature, while E_a is the activation energy for the viscous flow;
4. $\dot\gamma^*$ is the shear rate around the transition from Newtonian to plastic behavior;
5. The weighting functions $W_1(\dot\gamma)$ and $W_2(\dot\gamma)$ with $W_1(\dot\gamma)+W_2(\dot\gamma)=1$, must be continuous with continuous derivatives in order to ensure smooth transitions between two different behaviors;
6. $W_1(\dot\gamma)\gg W_2(\dot\gamma)$ for low shear rates (where Newtonian behavior is dominant), while $W_1(\dot\gamma)\ll W_2(\dot\gamma)$ for high shear rates (in which the plastic behavior prevails).

3.2. The experimental model in the pre-yield region

Model (47), in the pre-yield region, is equivalent to the Herschel–Bulkley model because $W_1(\dot\gamma)$ is negligible. However, around the yield point, the simple power-law expression of the Herschel–Bulkley part of the D.S. Resiga model is not sufficient to highlight the co-presence of elastic, viscous, and plastic behaviors for which this component cannot represent the evolutionary constitutive equations of the theoretical model (42). Therefore, it is necessary to generalize the Herschel–Bulkley component to obtain its $3D$ EVP version, which is able to model the evolution of τ through a system of evolutionary differential equations. This is possible in the GSM framework.

4. EVP fluids & GSMs

Constitutive equations for MR fluids must be objective [5] and must satisfy the second principle of thermodynamics. This is a difficult task, so we introduce GSMs as a robust and reliable framework in which MR fluids can be modeled meeting the two above-mentioned requirements.

4.1. GSM framework for constitutive equations

Remark 4.1. Firstly, we split the total deformation second-order tensor ϵ_{ij} into its elastic part, ϵ_{ij}^P, and its plastic part, ϵ_{ij}^P, $\epsilon_{ij}=\epsilon_{ij}^E+\epsilon_{ij}^P$. Defining the norm of a generic second-order tensor ϵ as the matrix norm by the square root of $\epsilon:\epsilon$, to give a greater understanding of the text, it appears useful to represent ϵ_{ij}, ϵ_{ij}^E, and ϵ_{ij}^P by the following matricial notations if the symbol $|\cdot|$ appears in the text: E, E^E, and E^P, respectively. Similarly, $\dot\epsilon_{ij}$, $\dot\epsilon_{ij}^E$, and $\dot\epsilon_{ij}^P$ are represented by $\dot{\mathrm{E}}$, $\dot{\mathrm{E}}^E$, and $\dot{\mathrm{E}}^P$, respectively.

Taking Remark 4.1 into account, a GSM, according to Halphen & Nguyen's approach [24], is completely defined by two convex functionals [7]:

1. The free energy of the system, $H(\epsilon_{ij},\epsilon_{ij}^E)=\omega|\mathrm{E}^E|^2$, where $|\mathrm{E}^E|^2=(\epsilon_{ij}^E:\epsilon_{ij}^E)$ and $\omega>0$, which represents the parameter of elasticity;
2. The potential for dissipation, $D(\dot\epsilon_{ij},\dot\epsilon_{ij}^E)=\underbrace{\varphi(\dot\epsilon_{ij})}_{\text{viscoelastic behavior}}+\underbrace{\varphi_p(\dot\epsilon_{ij}-\dot\epsilon_{ij}^E)}_{\text{viscoplastic behavior}}$, where $\varphi(\dot\epsilon_{ij})$ expresses the incompressible viscoelastic behavior and is associated with the viscosity ($\mu\geq 0$), while $\varphi(\dot\epsilon_{ij}P)$ expresses the viscoplastic behavior.[6] In particular, φ and φ_p can be expressed by [7,21,25]:

$$\varphi(\dot\epsilon_{ij})=\begin{cases}\mu|\dot{\mathrm{E}}|^2 & \text{if}\quad \dot\epsilon_{ii}=0\\ +\infty & \text{otherwise}\end{cases} \tag{48}$$

[5] That is, invariant by change of observers.

[6] φ_p expresses the viscoplastic behavior using a strictly positive power index ($n>0$), a consistency parameter K that is also positive, and a yield stress $\tau_0\geq 0$.

$$\varphi_p(\dot{\epsilon}^P_{ij}) = \varphi_p(\dot{\epsilon}_{ij} - \dot{\epsilon}^E_{ij}) = \begin{cases} \frac{2K}{n+1}|\dot{\mathrm{E}}^P|^{n+1} + \tau_0|\dot{\mathrm{E}}^P| & \text{if} \quad \dot{\epsilon}^P_{ii} = 0 \\ +\infty \quad \text{otherwise} \end{cases} \tag{49}$$

obtaining[7]:

$$\mathcal{D}(\dot{\epsilon}_{ij}, \dot{\epsilon}^E_{ij}) = \begin{cases} \mu|\dot{\mathrm{E}}|^2 + \frac{2K}{n+1}|\dot{\mathrm{E}}^P|^{n+1} + \tau_0|\dot{\mathrm{E}}^P| & \text{if} \quad \dot{\epsilon}^P_{ii} = 0 \\ +\infty \quad \text{otherwise.} \end{cases} \tag{50}$$

(48) and (49) are very important results of in-depth theoretical studies on the theory of complex fluids that have been confirmed by numerous practical laboratory experiments [7,21,25]. Moreover, the following result is valid, so the non-negativity and convexity of the functional $\mathcal{D}$ are guaranteed by the satisfaction of the second law of thermodynamics.

Proposition 4.2 *Convexity and Second Law of Thermodynamics Let us consider that $\mathcal{D} \geq 0$ and $\mathcal{D} = 0$ and that the heat flow is given by the Fourier law. Then, the second law of thermodynamics is satisfied.*

Proof. See [7]. □

4.2. The constitutive laws in the framework of GSM

Since materials with plasticity do not allow the calculation of the differential of $\mathcal{D}$ as φ and φ_p are not linear and cannot be differentiated, the writing of GSM constitutive equations involves the sub-differential of $\mathcal{D}$. So, we give the following definition:

Definition 1. Sub-differential of $\mathcal{D}$ Let us consider a bounded domain in $\mathbb{R}^N$, $N = 1, 2, 3$. The sub-differential of $\mathcal{D}$, indicated with $\partial\mathcal{D}$, represents the set of all directions of the straight lines passing through a point $\boldsymbol{\delta}_0$ of a curve that are below the curve itself. Formally,

$$\partial\mathcal{D}(\boldsymbol{\delta}_0) = \{\boldsymbol{\sigma} \in \mathbb{R}^{3\times3}_S; \ \ \partial\mathcal{D}(\boldsymbol{\delta}_0) + \boldsymbol{\sigma} : (\boldsymbol{\delta} - \boldsymbol{\delta}_0) \leq \mathcal{D}(\boldsymbol{\delta}), \quad \forall\boldsymbol{\delta} \in \mathbb{R}^{3\times3}_S\}$$

with $\mathbb{R}^{3\times3}_S$ representing the set of all symmetric matrices, 3×3.

In addition, the following important results are found.

Theorem 4.3. *Let $\mathcal{D}$ be a convex function. $\boldsymbol{\delta}_0$ is a minimum of $\mathcal{D}$ if and only if $0 \in \partial\mathcal{D}(\boldsymbol{\delta}_0)$. In other terms, $\boldsymbol{\delta}_0$ is a minimum point of $\mathcal{D}$ if and only if the straight line with no slope (indicated with 0) belong to its $\partial\mathcal{D}$.*

Then, as specified above, and according to the choice of both H and $\mathcal{D}$, the constitutive laws of the material are written as follows [7,21,25]:

$$\begin{cases} \tau_{ij} \in \frac{\partial H}{\partial \epsilon_{ij}} + \frac{\partial \mathcal{D}}{\partial \dot{\epsilon}_{ij}} \\ 0 \in \frac{\partial H}{\partial \epsilon^E_{ij}} + \frac{\partial \mathcal{D}}{\partial \dot{\epsilon}^E_{ij}} \end{cases} \tag{51}$$

where τ_{ij} is the total stress tensor. In addition, taking Eqs. (48) and (49) into account, the laws (51) assume the following form:

$$\begin{cases} \tau_{ij} \in \partial\varphi(\dot{\epsilon}_{ij}) + \partial\varphi_p(\dot{\epsilon}_{ij} - \dot{\epsilon}^E_{ij}) \\ 0 \in 2\omega\epsilon^E_{ij} - \partial\varphi_p(\dot{\epsilon}_{ij} - \dot{\epsilon}^E_{ij}). \end{cases} \tag{52}$$

Remark 4.4. Also, τ_{ij} is a second-order tensor whose deviatoric part is indicated by $(\tau_{ij})_d$. Then, the matrix norm of (τ_{ij}) and $(\tau_{ij})_d$, according to Remark 4.1, will be indicated by $|\mathrm{T}|$ and $|\mathrm{T}_d|$, respectively.

The following important result is worthwhile [7,21,25]:

Theorem 4.5. *Introducing the pressure p, the subdifferential $\partial\varphi(\dot{\epsilon}_{ij})$ is given by*

$$\partial\varphi(\dot{\epsilon}_{ij}) = \begin{cases} \{\tau_{ij}, \ \ \tau_{ij} = -p\delta_{ij} + 2\mu\dot{\epsilon}_{ij}\}, \quad \dot{\epsilon}_{ii} = 0 \\ \emptyset \quad \textit{otherwise.} \end{cases} \tag{53}$$

Taking into account both Remarks 4.1 and 4.4, the sub-differential $\partial\varphi_p(\dot{\epsilon}_{ij} - \dot{\epsilon}^E_{ij})$ assumes the form

$$\partial\varphi_p(\dot{\epsilon}_{ij} - \dot{\epsilon}^E_{ij}) = \begin{cases} \{\tau_{ij}, \ |T_d| \leq \tau_0\} \ \ \textit{if} \ \ \dot{\epsilon}_{ii} - \dot{\epsilon}^E_{ii} = 0 \\ \left\{\tau_{ij}, \quad \tau_{ij} = -p\delta_{ij} + 2K|\dot{E} - \dot{E}^E|^{n-1}(\dot{\epsilon}_{ij} - \dot{\epsilon}^E_{ij}) + \tau_0\frac{\dot{\epsilon}_{ij} - \dot{\epsilon}^E_{ij}}{|\dot{E} - \dot{E}^E|}\right\} \\ \qquad\qquad \textit{if} \ \ \dot{\epsilon}_{ij} - \dot{\epsilon}^E_{ij} \neq 0, \ \ \dot{\epsilon}_{ii} - \dot{\epsilon}^E_{ii} = 0 \\ \emptyset \quad \textit{otherwise} \end{cases} \tag{54}$$

where $(\tau_{ij})_d$ is the deviatoric part of τ_{ij}. In addition, the dual $\partial\varphi^*_p$ of $\partial\varphi_p$ is characterized by the Fenchel identity [7], according to which, for any $\tau_{ij} \in \partial\varphi_p(\dot{\epsilon}_{ij} - \dot{\epsilon}^E_{ij})$, by $\varphi^*_p(\tau_{ij}) = \tau_{ij} : (\dot{\epsilon}_{ij} - \dot{\epsilon}^E_{ij}) - \varphi_p(\dot{\epsilon}_{ij} - \dot{\epsilon}^E_{ij})$. In other terms, $\tau_{ij} \in \partial\varphi(\dot{\epsilon}_{ij} - \dot{\epsilon}^E_{ij})$ is equivalent to $\dot{\epsilon}_{ij} - \dot{\epsilon}^E_{ij} \in \partial\varphi^*_P(\tau_{ij})$. Again, from $\tau_{ij} + p\delta_{ij} = 2K|\dot{E} - \dot{E}^E|^{n-1}(\dot{\epsilon}_{ij} - \dot{\epsilon}^E_{ij}) + \tau_0\frac{\dot{\epsilon}_{ij} - \dot{\epsilon}^E_{ij}}{|\dot{E} - \dot{E}^E|}$ in (54), we obtain $|T_d| = 2K|\dot{E} - \dot{E}^E|^n + \tau_0$ so that $|\dot{E} - \dot{E}^E| = ((|T_d| - \tau_0)/(2K))^{1/n}$. Finally,

$$\partial\varphi^*_p(\tau_{ij}) = \left\{\dot{\epsilon}_{ij} - \dot{\epsilon}^E_{ij} \ \mid \ \dot{\epsilon}_{ij} - \dot{\epsilon}^E_{ij} = \max\left(0, \frac{|T_d| - \tau_0}{2K|T_d|^n}\right)^{1/n}(\tau_{ij})_d\right\}. \tag{55}$$

Proof. For details, see [7]. □

4.3. Evolutionary constitutive equations for elastoviscoplasticity

According to Theorem 4.5, the constitutive laws (52) can be written as follows:

$$\begin{cases} \tau_{ij} + p\delta_{ij} = 2\mu\dot{\epsilon}_{ij} + 2\omega\epsilon^E_{ij}, \quad \dot{\epsilon}_{ii} = 0 \\ \dot{\epsilon}_{ij} - \dot{\epsilon}^E_{ij} \in \partial\varphi^*_p(2\omega\epsilon^E_{ij}). \end{cases} \tag{56}$$

So, remembering that $\tau_{ij} = 2\omega\epsilon^E_{ij}$ [7], we obtain the following differential problem:

$$\frac{\dot{\tau}_{ij}}{2\omega} + \max\left(0, \frac{|\mathrm{T}_d| - \tau_0}{2K|\mathrm{T}_d|^n}\right)^{\frac{1}{n}}(\tau_{ij})_d = \dot{\epsilon}_{ij}. \tag{57}$$

As, in a large deformation regime[8] $\dot{\epsilon}_{ij} = D_{ij} = \frac{1}{2}(v_{i,j} + v_{j,i})$ and $\Omega_{ij} = \frac{1}{2}(v_{i,j} - v_{j,i})$ (vorticity tensor), system (57) becomes

$$\begin{cases} \rho\left(\frac{\partial v_i}{\partial t} + v_k v_{i,k}\right) - (-p\delta_{ik} + 2D_{ik} + \tau_{ik})_{,k} = \rho g_i \\ \frac{1}{\omega}\left(\frac{D_a\tau_{ij}}{Dt}\right)_d + \max\left(0, \frac{|\mathrm{T}| - \tau_0}{K|v_i|^n}\right)^{\frac{1}{n}}\tau_{ij} - 2D_{ij} = 0 \\ v_{i,i} = 0 \ \text{ in } \ (0,T)\times\Omega \\ \tau_{ij}(0) = (\tau_{ij})_0 \quad \wedge \quad v_i(t=0) = (v_i)_0 \quad \text{in} \ \ \Omega \\ \tau_{ij} = (\tau_{ij})_\Gamma \quad \wedge \quad v_i = (v_i)_\Gamma \quad \text{on} \ \ (0,T)\times\partial\Omega \end{cases} \tag{58}$$

where $\left(\frac{D_a\tau_{ij}}{Dt}\right)_d$ represents the Gordon–Schowalter derivative [26]:

$$\left(\frac{D_a\tau_{ij}}{Dt}\right)_d = \frac{\partial\tau_{ij}}{\partial t} + v_k\tau_{ij,k} + \tau_{ik}\Omega_{kj} - \Omega_{ik}\tau_{kj} - a(\tau_{ik}D_{kj} + D_{ik}\tau_{kj}) \tag{59}$$

in which $a \in [-1, 1]$ is the material parameter [7,21,25]. However, model (58) is not yet suitable for comparison with the theoretical model ((41) and (42)) due to the presence of the Gordon–Schowalter derivative, so we need to reformulate the problem in its dimensionless form and under the most frequent operating condition (simple shear flow). It is worth observing that in differential modeling, the Gordon–Schowalter derivative contributes to better fitting of the experimental dataset, especially when shear-thinning behavior takes place.

[7] $\dot{\mathrm{E}} = 0$ represents the condition of incompressibility of the fluid.

[8] Devices with MR fluids work under large deformations.

4.4. Dimensionless formulation and plasticity

Indicating, with V and L, respectively, the characteristic velocity and the length of the flow, let us introduce the following definitions [7,21,25]:

Definition 2. Viscosity π_p and Total Viscosity π_0:

$$\pi_p = K\left(\frac{L}{V}\right)^{1-n} \quad \pi_0 = \mu + \pi_p. \tag{60}$$

Definition 3. Relaxation Time, Characteristic Time of the Shear Flow, Characteristic Stress of the Flow and Slowdown Parameter:

$$\zeta = \frac{\pi_p}{\omega} \quad T = \frac{L}{V} \quad \Sigma = \frac{(\mu+\pi_p)V}{L} \quad \Pi = \pi_p/\pi_0 \in (0,1]. \tag{61}$$

Definition 4. Weissenberg, Bingham, and Reynolds Numbers:

$$We = \frac{\zeta V}{L} = \lambda\dot\gamma \quad Bi = \frac{\tau_0 L}{\pi_0 V} \quad Re = \frac{\rho V L}{\pi_0}. \tag{62}$$

If we take the above-defined parameters into account, problem (58) is reduced to the resolution of the following differential problem in the unknowns v_i, τ_{ij} and p [7,21]:

$$\begin{cases} Re\left(\frac{\partial v_i}{\partial t} + v_k v_{i,k}\right) - \frac{VL}{\pi_0}(-p\delta_{ik} + 2D_{ik} + \tau_{ik})_{,k} = \frac{VL}{\pi_0}\rho g_i \\ We\ \frac{D_a\tau_{ij}}{Dt} + k_n(|\mathrm{T}_d|)\tau_{ij} - 2\Pi D_{ij} = 0 \\ v_{i,i} = 0 \ \text{ in } \ (0,T)\times(-1,1) \\ \tau_{ij}(0) = (\tau_{ij})_0 \quad \wedge \quad v_i(t=0) = (v_i)_0 \ \text{ in } \ (-1,1) \\ \tau_{ij} = (\tau_{ij})_\Gamma \ \text{ on } \ \wedge \ \ v_i = (v_i)_\Gamma \quad (0,T)\times\partial(-1,1) \\ k_n(s) = \max\left(0,\ \frac{s-Bi}{(2\Pi)^{1-n}\,s^n}\right)^{1/n} \quad \forall s \geq 0 \end{cases} \tag{63}$$

where $k_n(s)$ represent the plasticity criteria function.

4.5. EVP model of simple shear flow

A *Simple Shear Flow* condition is established when, for $t = 0$, the fluid is at rest ($\tau_{ij}(0) = 0$) and, moreover, a constant shear rate in the rheometer direction, $\dot\gamma$, is applied. In this case, there is a $2D$ flow, and in addition,

$$We = \xi\dot\gamma, \quad Bi = \tau_0/(\pi_0\dot\gamma), \quad \nabla v_i = ([0,1];[0,0]), \quad s = |\mathrm{T}_d|. \tag{64}$$

Then, under these conditions, the system (63) is reduced to finding τ_{11}, τ_{22} and τ_{12} of τ, such that $\forall t > 0$ [7,21,25]:

$$\begin{cases} We\frac{d}{dt}\begin{pmatrix}\tau_{11}\\ \tau_{22}\\ \tau_{12}\end{pmatrix} + (We\mathcal{A}_a + k_n(|\mathrm{T}_d|)\mathrm{I})\begin{pmatrix}\tau_{11}\\ \tau_{22}\\ \tau_{12}\end{pmatrix} = \begin{pmatrix}0\\ 0\\ \Pi\end{pmatrix} \\ \tau_{ij}(0) = 0 \end{cases} \tag{65}$$

where I represents the identity matrix. Since

$$\mathcal{A}_a = \begin{pmatrix} 0 & 0 & -(1+a) \\ 0 & 0 & 1-a \\ \frac{1-a}{2} & -\frac{1+a}{2} & 0, \end{pmatrix} \tag{66}$$

we obtain

$$We\mathcal{A}_a + k_n(|\mathrm{T}_d|)\mathrm{I} = \begin{pmatrix} k_n(|\mathrm{T}_d|) & 0 & -\zeta\dot\gamma(1+a) \\ 0 & k_n(|\mathrm{T}_d|) & \zeta\dot\gamma(1-a) \\ \zeta\dot\gamma\frac{1-a}{2} & -\zeta\dot\gamma\frac{1+a}{2} & k_n(|\mathrm{T}_d|) \end{pmatrix}. \tag{67}$$

Then, (65) becomes

$$\begin{cases} \zeta\dot\gamma\frac{d}{dt}\begin{pmatrix}\tau_{11}\\ \tau_{22}\\ \tau_{12}\end{pmatrix} + \begin{pmatrix} k_n(|\mathrm{T}_d|) & 0 & -\zeta\dot\gamma(1+a) \\ 0 & k_n(|\mathrm{T}_d|) & \zeta\dot\gamma(1-a) \\ \zeta\dot\gamma\frac{1-a}{2} & -\zeta\dot\gamma\frac{1+a}{2} & k_n(|\mathrm{T}_d|) \end{pmatrix}\begin{pmatrix}\tau_{11}\\ \tau_{22}\\ \tau_{12}\end{pmatrix} = \begin{pmatrix}0\\ 0\\ \Pi\end{pmatrix} \\ \tau_{ij}(0) = 0 \end{cases} \tag{68}$$

or equivalently,

$$\begin{cases} \zeta\dot\gamma\frac{d\tau_{11}}{dt} + k_n(|\mathrm{T}_d|)\tau_{11} - \zeta\dot\gamma(1+a)\tau_{12} = 0 \\ \zeta\dot\gamma\frac{d\tau_{22}}{dt} + k_n(|\mathrm{T}_d|)\tau_{22} + \zeta\dot\gamma(1-a)\tau_{12} = 0 \\ \zeta\dot\gamma\frac{d\tau_{12}}{dt} + \zeta\dot\gamma\frac{1-a}{2}\tau_{11} - \zeta\dot\gamma\frac{1+a}{2}\tau_{22} + k_n(|\mathrm{T}_d|)\tau_{12} = \Pi \\ \tau_{ij}(0) = 0. \end{cases} \tag{69}$$

5. Correspondence between the Chen & Yeh mixture model and the D.S. Resiga Model: The details

Before detailing the correspondence between the theoretical and experimental models, we need to establish some operating conditions. For this purpose, let us introduce Proposition 5.1 with Remarks 5.2 and 5.3, which are useful for the following part of the paper.

Proposition 5.1. *The solution to problem (69) in simple shear flow and for $t \to +\infty$ tends to a constant value (for $Bi \geq 0$). In addition, if $n \leq 1$, τ_{12} significantly decreases (as t increases).*

Proof. See [7,25]. □

Under usual industrial operating conditions and in a simple shear flow regime, the time is sufficiently long and, moreover, for the materials governed by the Herschel–Bulkley EVP models, Proposition 5.1 is yielded, showing that τ_{12}, under the same conditions, can be considered negligible. Then, in accordance with Proposition 5.1, system (79) is simplified as follows:

$$\begin{cases} \zeta\dot\gamma\frac{d\tau_{11}}{dt} + k_n(|\mathrm{T}_d|)\tau_{11} = 0 \\ \zeta\dot\gamma\frac{d\tau_{22}}{dt} + k_n(|\mathrm{T}_d|)\tau_{22} = 0 \\ \zeta\dot\gamma\frac{1-a}{2}\tau_{11} - \zeta\dot\gamma\frac{1+a}{2}\tau_{22} = \Pi \\ \tau_{ii}(0) = 0. \end{cases} \tag{70}$$

5.1. Some useful remarks

Remark 5.2. From system (63), we have $k_n(s) = \max\left(0,\ \frac{s-Bi}{(2\Pi)^{1-n}\,s^n}\right)^{1/n}$, $\forall s \geq 0$. Then, taking into account that $n \geq 0$, $\Pi = \frac{\pi_p}{\pi_0} \in (0,1]$ and $\pi_0 = \mu + \pi_p$, the following two cases may occur:

1.
$$\frac{s - B_i}{(2\Pi)^{1-n}s^n} > 0 \tag{71}$$

2.
$$\frac{s - B_i}{(2\Pi)^{1-n}s^n} \leq 0. \tag{72}$$

If inequality (72) occurs, $k_n(s) = 0$, considering (70), we can write

$$\begin{cases} \frac{d\tau_{11}}{dt} = \frac{d\tau_{22}}{dt} = 0 \\ \zeta\dot\gamma\frac{1-a}{2}\tau_{11} - \zeta\dot\gamma\frac{1+a}{2}\tau_{22} = \Pi \\ \tau_{ii}(0) = 0 \end{cases} \tag{73}$$

obtaining that τ_{11} and τ_{22} are both null. In other words, even if the MR fluid was subjected to **H**, it would not develop shear stress, establishing an unacceptable physical condition. Then, we yield inequality (71) so we can write

$$\max\left(0,\ \frac{s - Bi}{(2\Pi)^{1-n}\,s}\right) = \frac{s - Bi}{(2\Pi)^{1-n}\,s} \tag{74}$$

from which

$$k_n(s) = \max\left(0,\ \frac{s - Bi}{(2\Pi)^{1-n}s^n}\right)^{\frac{1}{n}} = \sqrt[n]{\frac{s - Bi}{(2\Pi)^{1-n}s^n}}. \tag{75}$$

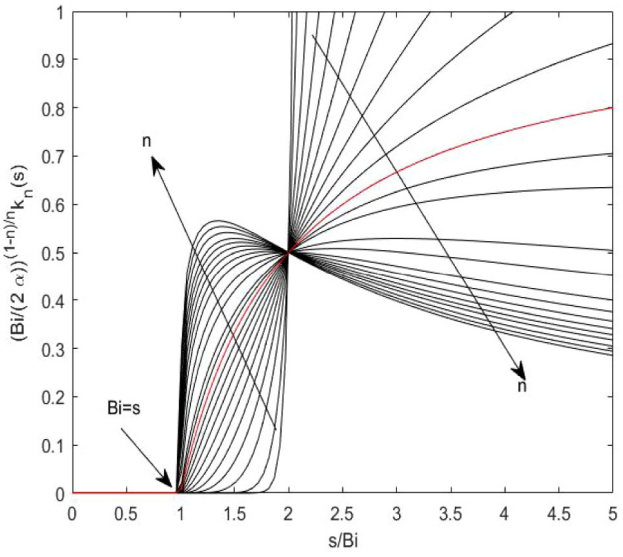

Fig. 1. HB EVP: the plasticity criteria function $k_n(s)$ for increasing values of n. The red line refers to $n = 1$.

Remark 5.3. It is interesting to make the scaling version of (75). In other words,

$$k_n(s) = \left(\frac{Bi(\frac{s}{Bi} - 1)}{Bi^n (2\Pi)^{1-n} (\frac{s}{Bi})^n} \right)^{\frac{1}{n}} = \left(\frac{Bi}{2\Pi} \right)^{\frac{1-n}{n}} \left(\frac{\frac{s}{Bi} - 1}{(\frac{s}{Bi})^n} \right)^{\frac{1}{n}}, \tag{76}$$

from which

$$\left(\frac{Bi}{2\Pi} \right)^{\frac{n-1}{n}} k_n(s) = \left(\frac{\frac{s}{Bi} - 1}{(\frac{s}{Bi})^n} \right)^{\frac{1}{n}}. \tag{77}$$

Fig. 1 displays $k_n(s)$ versus s/Bi, highlighting different behaviors depending on the operative conditions for various values of n (shear-thinning or shear-thickening) (see also [21,25]). It is easy to observe that, if $n < 1$, the function is continuous with both its left and right derivatives being equal to zero. Then, the function is smooth for $n < 1$. Conversely, for $n > 1$ and $\frac{s}{Bi} < 2$, the function is not smooth. These differences are displayed in Table 3. In particular, to ensure the smoothing behavior of $k_n(s)$ for each s, we need to establish a shear-thinning regime ($n < 1$) for industrial applications. Moreover, if $\frac{s}{Bi} < 2$, taking into the definition of the Bingham number, we have

$$s < \frac{2\tau_0}{\pi_0 \dot{\gamma}}. \tag{78}$$

In other words, when establishing a fixed value of τ_0, [9] s becomes bounded. Otherwise, if $\frac{s}{Bi} > 2$, it follows that $s > \frac{2\tau_0}{\pi_0 \dot{\gamma}}$, so s becomes unbounded, proving to be uncontrollable. Now, we focus our attention on $\frac{s}{Bi} < 2$, highlighting that $k_n(s) < k_1(s)$. This means that, under the above conditions, $k_1(s)$ represents a sort of upper-bound condition of plasticity.

In our study $s = |\mathrm{T}_d|$, for the reasons explained in Remark 5.3, we formalize the correspondence between the theoretical model and the experimental one by means of $k_1(|\mathrm{T}_d|)$. Then, system (70) can be written as follows:

$$\begin{cases} \zeta\dot{\gamma} \frac{d\tau_{11}}{dt} + k_1(|\mathrm{T}_d|)\tau_{11} = 0 \\ \zeta\dot{\gamma} \frac{d\tau_{22}}{dt} + k_1(|\mathrm{T}_d|)\tau_{22} = 0 \\ \zeta\dot{\gamma} \frac{d\tau_{12}}{dt} + \zeta\dot{\gamma} \frac{1-a}{2} \tau_{11} - \zeta\dot{\gamma} \frac{1+a}{2} \tau_{22} = \Pi \\ \tau_{ij}(0) = 0. \end{cases} \tag{79}$$

[9] That is, establishing the intended use of the manufacture.

The following Proposition suggests how to write the plasticity criteria function under the chosen operating conditions.

Proposition 5.4. *Under shear-thinning conditions and for* $n = 1$, $k_1(|T_d|)\tau_{ij} = \tau_{ij} - \frac{Bi}{|T_d|}\tau_{ij}$.

Proof. By multiplying both sides of (75) by τ_{ij} and taking into account that in our case, $s = k_n(|\mathrm{T}_d|)$, we have[10]:

$$\begin{aligned} k_n(|\mathrm{T}_d|)\tau_{ij} &= \left(\frac{(|\mathrm{T}_d| - Bi)}{(2\Pi)^{1-n} |\mathrm{T}_d|^n} \right)^{1/n} \tau_{ij} = \frac{1}{|\mathrm{T}_d|} \frac{(|\mathrm{T}_d| - Bi)^{\frac{1}{n}}}{(2\Pi)^{\frac{1-n}{n}}} \tau_{ij} \\ &= \frac{(2\Pi)^{\frac{n-1}{n}}}{|\mathrm{T}_d|} \left(|\mathrm{T}_d| - Bi \right)^{\frac{1}{n}} \tau_{ij} \end{aligned} \tag{80}$$

from which, taking Remark 5.3 (that is, $n = 1$) into account, we obtain

$$k_1(|\mathrm{T}_d|)\tau_{ij} = \frac{1}{|\mathrm{T}_d|} (|(\tau_{ij})_d| - Bi)\tau_{ij} = \tau_{ij} - \frac{Bi}{|\mathrm{T}_d|}\tau_{ij}. \quad \square \tag{81}$$

It is important to underline the fact that system (70) (although in a simplified version) governs fluids through the Herschel–Bulkley formulation in the framework of the GSM. So, it makes sense to rewrite (70) in the following form:

$$\begin{cases} \zeta\dot{\gamma} \frac{d\tau_{11}^F}{dt} + k_1(|\mathrm{T}_d|)\tau_{11}^F = 0 \\ \zeta\dot{\gamma} \frac{d\tau_{22}^F}{dt} + k_1(|\mathrm{T}_d|)\tau_{22}^F = 0 \\ \frac{\zeta\dot{\gamma}}{\Pi} \frac{1-a}{2} \tau_{11}^F - \frac{\zeta\dot{\gamma}}{\Pi} \frac{1+a}{2} \tau_{22}^F = 1 \\ \tau_{ij}(0) = 0 \end{cases} \tag{82}$$

which, taking into account the decomposition (15) and supposing that p^F is constant, can be written as

$$\begin{cases} \zeta\dot{\gamma} \frac{d\tau_{11}^{FS}}{dt} + \zeta\dot{\gamma} \frac{d\tau^{FB}}{dt} = -k_1(|\mathrm{T}_d|)\tau_{11}^{FS} - k_1(|\mathrm{T}_d|)\tau^{FB} + k_1(|\mathrm{T}_d|)p^F \\ \zeta\dot{\gamma} \frac{d\tau_{22}^{FS}}{dt} + \zeta\dot{\gamma} \frac{d\tau^{FB}}{dt} = -k_1(|\mathrm{T}_d|)\tau_{22}^{FS} - k_1(|\mathrm{T}_d|)\tau^{FB} + k_1(|\mathrm{T}_d|)p^F \\ \frac{\zeta\dot{\gamma}}{\Pi} \frac{1-a}{2} \tau_{11}^F - \frac{\zeta\dot{\gamma}}{\Pi} \frac{1+a}{2} \tau_{22}^F = 1 \\ \tau_{ij}(0) = 0 \end{cases} \tag{83}$$

and by separating the contributions due to FS and FB, we can write

$$\begin{cases} \zeta\dot{\gamma} \frac{d\tau_{11}^{FS}}{dt} = -k_1(|\mathrm{T}_d|)\tau_{11}^{FS} + k_1(|\mathrm{T}_d|)p^F \\ \zeta\dot{\gamma} \frac{d\tau_{22}^{FS}}{dt} = -k_1(|\mathrm{T}_d|)\tau_{22}^{FS} + k_1(|\mathrm{T}_d|)p^F \\ \zeta\dot{\gamma} \frac{d\tau^{FB}}{dt} = -k_1(|\mathrm{T}_d|)\tau^{FB} \\ \frac{\zeta\dot{\gamma}}{\Pi} \frac{1-a}{2} \tau_{11}^F - \frac{\zeta\dot{\gamma}}{\Pi} \frac{1+a}{2} \tau_{22}^F = 1 \\ \tau_{ij}(0) = 0. \end{cases} \tag{84}$$

Now, let us proceed with the comparison between system (84) and system (46). In other words, the following results are valid.

Proposition 5.5. *The terms* $\zeta\dot{\gamma} \frac{d\tau_{11}^{FS}}{dt}$, $\zeta\dot{\gamma} \frac{d\tau_{22}^{FS}}{dt}$, *and* $\zeta\dot{\gamma} \frac{d\tau^{FB}}{dt}$ *in the system (84) correspond, qualitatively, to the terms* $\lambda_4 \mu^S \frac{d\tau_{11}^{FS}}{dt}$, $\lambda_4 \mu^S \frac{d\tau_{22}^{FS}}{dt}$ *and* $\lambda_5 \mu^B \frac{d\tau^{FB}}{dt}$ *in system (46).*

Proof. Taking into account the first equation in (60) and the first equation in (61), the terms $\zeta\dot{\gamma} \frac{d\tau_{11}^{FS}}{dt}$, $\zeta\dot{\gamma} \frac{d\tau_{22}^{FS}}{dt}$, and $\zeta\dot{\gamma} \frac{d\tau^{FB}}{dt}$ in (84) can be easily written as follows:

$$\zeta\dot{\gamma} \frac{d\tau_{11}^{FS}}{dt} = \frac{\dot{\gamma}}{\omega} \underbrace{K \left(\frac{L}{V} \right)^{1-n}}_{\text{viscosity}} \frac{d\tau_{11}^{FS}}{dt}; \tag{85}$$

[10] This is possible because $k_n(|\mathrm{T}_d|)$ is a scalar.

Table 3
Function criteria of plasticity $k_n(s)$: characteristics of smoothing for different fluid behaviors (shear-thinning and shear-thickening).

	$\frac{s}{Bi} < 2$	$\frac{s}{Bi} > 2$
$n > 1$ (shear-thickening)	$k_n(s) > k_1(s)$ no smooth	$k_n(s) < k_1(s)$ smooth
$n < 1$ (shear-thinning)	$k_n(s) < k_1(s)$ smooth	$k_n(s) > k_1(s)$ smooth

$$\zeta \frac{d\tau_{22}^{FS}}{dt} = \frac{\dot\gamma}{\omega} \underbrace{K\left(\frac{L}{V}\right)^{1-n}}_{\text{viscosity}} \frac{d\tau_{22}^{FS}}{dt};$$

$$\zeta\dot\gamma \frac{d\tau^{FB}}{dt} = \frac{\dot\gamma}{\omega} \underbrace{K\left(\frac{L}{V}\right)^{1-n}}_{\text{viscosity}} \frac{d\tau^{FB}}{dt}$$

where it is observed that $K\left(\frac{L}{V}\right)^{1-n}$ is a viscosity. In addition, with $\dot\gamma$ being the shear rate, it can be considered a function of the mechanical tension and, consequently, $\frac{\dot\gamma}{\omega}$ in (85) represents a function of the deformations. On the other hand, in the terms

$$\lambda_4\mu^S \frac{d\tau_{11}^{FS}}{dt}; \quad \lambda_4\mu^S \frac{d\tau_{22}^{FS}}{dt}; \quad \lambda_5\mu^B \frac{d\tau^{FB}}{dt} \tag{86}$$

present in (46), λ_4 and λ_5 are characterized by the following explicit functional dependence (for details, see system (33)):

$$\begin{cases} \lambda_4 = \lambda_4(\rho^F, \theta, e_{ij}^{SE}) \\ \lambda_5 = \lambda_5(\rho^F, \theta, e_{ij}^{SE}) \end{cases} \tag{87}$$

where e_{ij}^{SE} represents the Eulerian elastic strain tensor. Then, the terms (86) become

$$\lambda_4(\rho^F, \theta, e_{ij}^{SE}) \underbrace{\mu^S}_{\text{viscosity}} \frac{d\tau_{11}^{FS}}{dt}; \quad \lambda_4(\rho^F, \theta, e_{ij}^{SE}) \underbrace{\mu^S}_{\text{viscosity}} \frac{d\tau_{22}^{FS}}{dt}; \tag{88}$$

$$\lambda_5(\rho^F, \theta, e_{ij}^{SE}) \underbrace{\mu^B}_{\text{viscosity}} \frac{d\tau^{FB}}{dt}.$$

It is worth noting that the viscous terms explicitly appear in (85) and (88) thanks to the factors $K\left(\frac{L}{V}\right)^{1-n}$, μ^S and μ^B, respectively. Moreover, $\frac{d\tau_{11}^{FS}}{dt}$, $\frac{d\tau_{22}^{FS}}{dt}$ and $\frac{d\tau^{FB}}{dt}$ are also explicit in (85) and (88). Finally, the functional dependency of the deformation in $\frac{\dot\gamma}{\omega}$ (see (85)) is present in relation (88) by means of $\lambda_4(\rho^F, \theta, e_{ij}^{SE})$ and $\lambda_5(\rho^F, \theta, e_{ij}^{SE})$. □

Proposition 5.6. *The term $-k_1(|T_d|)\tau^{FB}$, which appears in system (84), qualitatively corresponds to the terms $-\tau^{FB} + \mu^B v_{1,1}^F + \mu^B v_{2,2}^F$ in system (46).*

Proof. By means of (81), we can write

$$-k_1(|T_d|)\tau^{FB} = -\tau^{FB} + \frac{Bi}{|T_d|}\tau^{FB}. \tag{89}$$

Since Bi represents the stress yield divided by the viscous stress, the term $\frac{Bi}{|T_d|}\tau^{FB}$ in (89) can be qualitatively considered as the amount of stress tension related to the fluid deriving from the fluid bulk (in shear-thinning behavior). In other words, qualitatively, $\frac{Bi}{|T_d|}$ can be considered to correspond to $\mu^B v_{1,1}^F + \mu^B v_{2,2}^F$. □

Proposition 5.7. *The terms $-k_1(|T_d|)\tau_{11}^{FS} + k_1(|T_d|)p^F$ and $-k_1(|T_d|)\tau_{22}^{FS} + k_1(|T_d|)p^F$ in the system (84) correspond, qualitatively, to $-\tau_{11}^{FS} + \mu^S D_{11}^F$ and $-\tau_{22}^{FS} + \mu^S D_{22}^F$ in (46), respectively.*

Proof. Exploiting (81) one more time, we can write (for $n = 1$)

$$-k_1(|T_d|)\tau_{11}^{FS} = -\tau_{11}^{FS} + \frac{Bi}{|T_d|}\tau_{11}^{FS} \tag{90}$$

and

$$k_1(|T_d|)p^F = \left(1 - \frac{Bi}{|T_d|}\right)p^F. \tag{91}$$

Then, taking into account both (90) and (91), we can write

$$-k_1(|T_d|)\tau_{11}^{FS} + k_1(|T_d|)p^F = -\tau_{11}^{FS} + \frac{Bi}{|T_d|}\tau_{11}^{FS} + \left(1 - \frac{Bi}{|T_d|}\right)p^F. \tag{92}$$

In addition, by exploiting the decomposition (15), (92) becomes

$$-k_1(|T_d|)\tau_{11}^{FS} + k_1(|T_d|)p^F = -\tau_{11}^{FS} + \frac{Bi}{|T_d|}\tau_{11}^{FS} + p^F\left(1 - \frac{Bi}{|T_d|}\right) = \tag{93}$$

$$= -\tau_{11}^{FS} + \frac{Bi}{|T_d|}(\tau_{11}^F + p^F - \tau^{FB}) + p^F\left(1 - \frac{Bi}{|T_d|}\right) =$$

$$= -\tau_{11}^{FS} + \frac{Bi}{|T_d|}\left(\tau_{11}^F - \tau^{FB} + \frac{|T_d|}{Bi}p^F\right)$$

and, in a similar way, we achieve

$$-\tau_{22}^{FS} + \frac{Bi}{|T_d|}\left(\tau_{22}^F - \tau^{FB} + \frac{|T_d|}{Bi}p^F\right). \tag{94}$$

We observe that, in (93), $\tau_{11}^F - \tau^{FB} + \frac{|T_d|}{Bi}p^F$, being a "net" mechanical tension along a specific direction, can be considered proportional to the gradient of the velocity of the fluid in the same direction. Then, the term $\frac{Bi}{|T_d|}\left(\tau_{11}^F - \tau^{FB} + \frac{|T_d|}{Bi}p^F\right)$ in (93) qualitatively corresponds to $\mu^S D_{11}^F$ in (46). Analogously, the term $\frac{Bi}{|T_d|}\left(\tau_{22}^F - \tau^{FB} + \frac{|T_d|}{Bi}p^F\right)$ in (94) qualitatively corresponds to $\mu^S D_{22}^F$ in (46), from which the thesis follows. □

Proposition 5.8. *The information content present in the third equation of the system (84) is contained, in the pre-yield region, in the dissipative inequality of the Chen theoretical model (that is, (41)).*

Proof. Considering the third equation in the system (84), by means of decomposition (15), it becomes

$$\left(\frac{1-a}{2}\right)(\tau_{11}^{FS} - p^F + \tau^{FB}) - \left(\frac{1+a}{2}\right)(\tau_{22}^{FS} - p^F + \tau^{FB}) = \frac{\Pi}{\zeta\dot\gamma} \tag{95}$$

from which, after simple algebraic calculations, we achieve

$$\frac{\tau_{22}^{FS} - \tau_{11}^{FS}}{2} + a\frac{\tau_{22}^{FS} + \tau_{11}^{FS}}{2} + a\tau^{FB} = ap^F - \frac{\Pi}{\zeta\dot\gamma} \tag{96}$$

and again,

$$\tau_{22}^{FS}(1+a) - \tau_{11}^{FS}(1-a) + 2a\tau^{FB} = 2ap^F - 2\frac{\Pi}{\zeta\dot\gamma}, \tag{97}$$

from which

$$-\tau_{11}^{FS}(1-a) + a\tau^{FB} + \tau_{22}^{FS}(1+a) + a\tau^{FB} = ap^F - \frac{\Pi}{\zeta\dot\gamma} + ap^F - \frac{\Pi}{\zeta\dot\gamma}. \tag{98}$$

Moreover, by separating the contributions in (98) we can write

$$\begin{cases} -\tau_{11}^{FS}(1-a) + a\tau^{FB} = ap^F - \frac{\Pi}{\zeta\dot\gamma} \\ \tau_{22}^{FS}(1+a) + a\tau^{FB} = ap^F - \frac{\Pi}{\zeta\dot\gamma}, \end{cases} \tag{99}$$

which becomes

$$\begin{cases} -\tau_{11}^{FS}(1-a) + a\tau^{FB} = ap^F - \frac{\Pi}{\zeta\dot\gamma} \\ -\tau_{22}^{FS}(-1-a) + a\tau^{FB} = ap^F - \frac{\Pi}{\zeta\dot\gamma}. \end{cases} \tag{100}$$

On the other hand, inequality (41), taking into account Remark 2.2, can be easily rewritten as follows:

$$-\tau_{ij}^{FS}\left(\lambda_4\frac{d\tau_{ij}^{FS}}{dt} - D_{ij}^F\right) + \tau^{FB}\left(v_{i,i}^F - \lambda_5\frac{d\tau^{FB}}{dt}\right) \geq 0. \tag{101}$$

Table 4
Mixture Model & HB EVP Model: qualitative correspondence among terms in the pre-yield region and shear-thinning behavior.

D.S. Resiga Model (see system (84))	Chen & Yeh Mixture Model (see system (46) and inequality (41))
$\zeta\dot{\gamma}\frac{d\tau_{11}^{FS}}{dt}$	$\lambda_4\mu^S\frac{d\tau_{11}^{FS}}{dt}$
$\zeta\dot{\gamma}\frac{d\tau_{22}^{FS}}{dt}$	$\lambda_4\mu^S\frac{d\tau_{22}^{FS}}{dt}$
$\zeta\dot{\gamma}\frac{d\tau^{FB}}{dt}$	$\lambda_5\mu^B\frac{d\tau^{FB}}{dt}$
$-k_1(\lvert\mathrm{T}_d\rvert)\tau_{11}^{FS}+k_1(\lvert\mathrm{T}_d\rvert)p^F$	$-\tau_{11}^{FS}+\mu^S D_{11}^F$
$-k_1(\lvert\mathrm{T}_d\rvert)\tau_{22}^{FS}+k_1(\lvert\mathrm{T}_d\rvert)p^F$	$-\tau_{22}^{FS}+\mu^S D_{22}^F$
$-k_1(\lvert\mathrm{T}_d\rvert)\tau^{FB}$	$-\tau^{FB}+\mu^B v_{1,1}^F+\mu^B v_{2,2}^F$

It is known that a, in the Gordon–Schowalter time derivative (see (59)), takes into account the contributions due to the symmetric part of the velocity gradient tensor. Then, in our case, this tensor has to be referred to the fluid continuum (that is, D_{ij}^F). Then, qualitatively, the factors $(1-a)$ and $(-1-a)$ in (100) can be considered to correspond to the factors $\left(\lambda_4\frac{d\tau_{11}^{FS}}{dt}-D_{11}^F\right)$ and $\left(\lambda_4\frac{d\tau_{22}^{FS}}{dt}-D_{22}^F\right)$ in (101), respectively. Moreover, since $D_{ij}^F=\frac{1}{2}(v_{i,j}^F+v_{j,i}^F)$, it follows that factor a in (100) can be considered qualitatively correspondent to $\left(v_{i,i}^F-\lambda_5\frac{d\tau^{FB}}{dt}\right)$ in (101). Then, it is shown that the information content present in (97) is contained in inequality (101), from which the thesis follows. □

Therefore, Propositions 5.1, 5.4, 5.5, 5.6, 5.7, and 5.8, together Remarks 5.2 and 5.3, formalize the qualitative correspondence between the EVP experimental model and the theoretical model. The obtained correspondences are summarized in Table 4. It is worth emphasizing that, after this study, it is possible to use a simplified experimental version (and therefore easily implemented) of the theoretical approach characterized by prohibitive computational costs. However, it is possible to formalize this qualitative correspondence between the models by taking into account the statement of Proposition 5.1, according to which, under the assumed operating conditions, the terms containing τ_{12} in the experimental model (see, system (69)) can be neglected. This simplification produces an inevitable loss of information content, whatever the low power index, n, is. Section 6 deals with the assessment (qualitative) of the effects derived from this simplification by means of some numerical tests, and these results are compared with those of two well-known benchmarks from the literature [21].

6. Some significant tests

In this section, we present two numerical tests that are achieved by fixing particular values of Bi, a, We, and Π and varying n, as reported by two well-known benchmarks from the literature [25]. The implementations were made using Matlab® (Release 2017a) by means of Runge–Kutta techniques. The following Remark was particularly useful.

Remark 6.1. By exploiting Proposition 5.1, the following equation can be obtained [21]:

$$\lvert\mathrm{T}_d\rvert^2=\frac{1}{2}(\tau_{11}-\tau_{22})^2+2\tau_{12}^2=\frac{1}{2}(\tau_{11}-\tau_{22})^2. \tag{102}$$

In addition, due to the isotropic pressure contribution, p^F, it is not possible to directly measure both τ_{11} and τ_{22}. What can be measured is the difference between these quantities as the pressure elides. Then, after introducing the new variable $\psi=\frac{\tau_{11}-\tau_{22}}{2}$, we can write

$$k_n(\lvert\mathrm{T}_d\rvert)=\frac{\sqrt[n]{\sqrt{2}\psi-Bi}}{\sqrt[n]{(2\Pi)^{1-n}(\sqrt{2})^n\psi^n}}. \tag{103}$$

It is worth noting that the experimental data have always shown a positive value of $\tau_{11}--\tau_{22}$ [7,25], so ψ is always positive. In accordance with (70), the second equation is subtracted from the first one, and taking into account (103), we obtain the following Cauchy's problem:

$$\begin{cases}\frac{d\psi}{dt}=-\frac{\sqrt[n]{\sqrt{2}\psi-Bi}}{\zeta\dot{\gamma}2^{\frac{2-n}{2n}}\Pi^{\frac{1-n}{n}}}\\ \psi(0)=0\end{cases} \tag{104}$$

which has a unique solution, since the function $-\frac{\sqrt[n]{\sqrt{2}\psi-Bi}}{\zeta\dot{\gamma}2^{\frac{2-n}{2n}}\Pi^{\frac{1-n}{n}}}$ and its first derivative are continuous functions that ensure the absence of ghost solutions in the numerical tests. We also observe that, by means of the usual techniques of integrations of ordinary differential equations, the analytical solution of (104) can be written as follows:

$$\psi(t)=\frac{\sqrt{2}}{2}\left(\left(\frac{2}{\dot{\gamma}}\right)^{\frac{n}{-1+n}}\times\left(\left(\frac{\sqrt[n]{2}\zeta\, n}{(1-n)\Pi^{\frac{-1+n}{n}}}\left(-\frac{Bi\dot{\gamma}\sqrt[n]{2}\zeta n}{2(-1+n)\Pi^{\frac{-1+n}{n}}}+t\right)^{-1}\right)^{\frac{n}{-1+n}}\right)^{-1}+Bi\right) \tag{105}$$

whose structure is not very suitable for industrial applications. Then, we carry out numerical tests to achieve some interesting results of industrial interest.

6.1. Case 1: Simple shear flow for $\mathbf{a=We=Bi=\Pi=1}$

The evolution of $\psi(t)$ in (104), starting from $\psi(0)=0$[11] for $Bi=a=We=\Pi=1$ and in the presence of shear-thinning behavior ($n<1$) is shown in Fig. 2(a) when n increases. The achieved solutions monotonically increase and tend toward a constant value when $t\to+\infty$, so that, for a sufficiently long t, the highlighted evolution overlaps with the well-known literature benchmarks [21]. However, in comparison with the results obtained in [21], in all of the cases considered, the transitory phenomenon evolves with a lower time constant so that, in this study, the fluid responds faster to the stress compared to when τ_{12} has not been neglected [21]. To emphasize this aspect, Fig. 3(a) displays a suitable zoomed in version of Fig. 2(a), also highlighting that, starting from $t=0$, the solution for $n=1$ does not represent the upper-bound solution (region A in Fig. 3(a)), while in region B, this condition is restored. The reduced time constant values are due to the fact that the model (70) is simplified with respect to (69) so the missing terms in (70) produced in [21] delay the response. In addition, the absence of τ_{12} in (70) does not allow us to highlight any fluctuations at the start of evolution. The same simplification, on the other hand, produces an effect on τ_{22}. In fact, using the third equation of the system (70), for $a=1$, we obtain $\tau_{22}=-\frac{\Pi}{\zeta\dot{\gamma}}$, from which it is clear that, under the same operating conditions, τ_{22} is a constant value.

6.2. Case 2: Simple shear flow for $\mathbf{a=0}$, $\mathbf{We=Bi=\Pi=1}$

As for Case 1, the evolution of $\psi(t)$ in (104) with a null initial condition is displayed in Fig. 2(b) for an increasing n and $a=0$, $We=Bi=\Pi=1$. Also, in this case, the monotonically increasing behavior was confirmed under the same conditions in [21], showing a tendency to move toward a constant value for $t\to+\infty$, whatever the values of Bi and n are. As in the previous case, the time constant is reduced compared to the one obtained in [21], with consequent achievement of the regime condition in a reduced amount of time. Moreover, also in this case, the absence of τ_{12}^F in (70) produces a strong decay in the fluctuations in the initial phase. The zoom displayed in Fig. 3(b) also highlights that the solution for $n=1$ in the right neighborhood of

[11] In other terms, it is supposed that the MR fluid is stressed starting from the rest condition, when $t=0$.

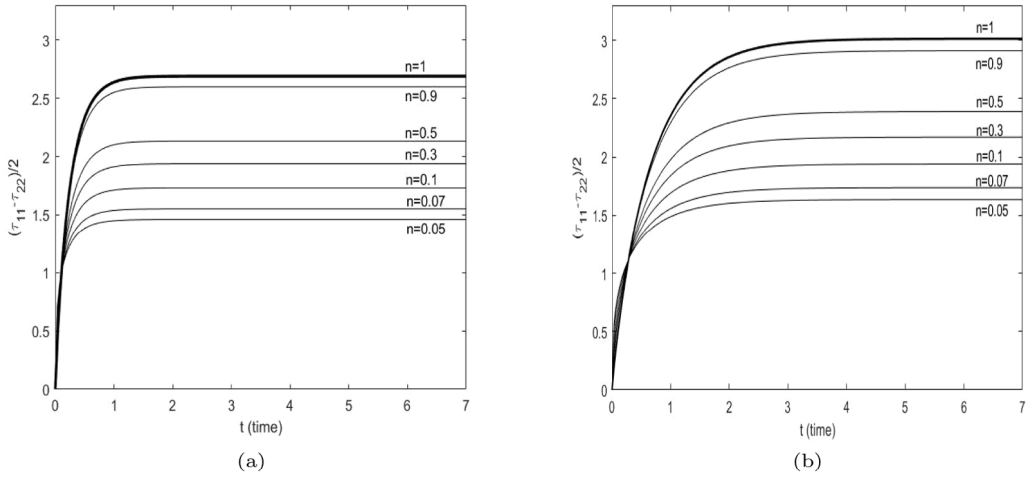

Fig. 2. As n increases, the $\psi(t)$ evolution with $Bi = We = \Pi = 1$ is as follows: (a) when $a = 1$; (b) $a = 0$.

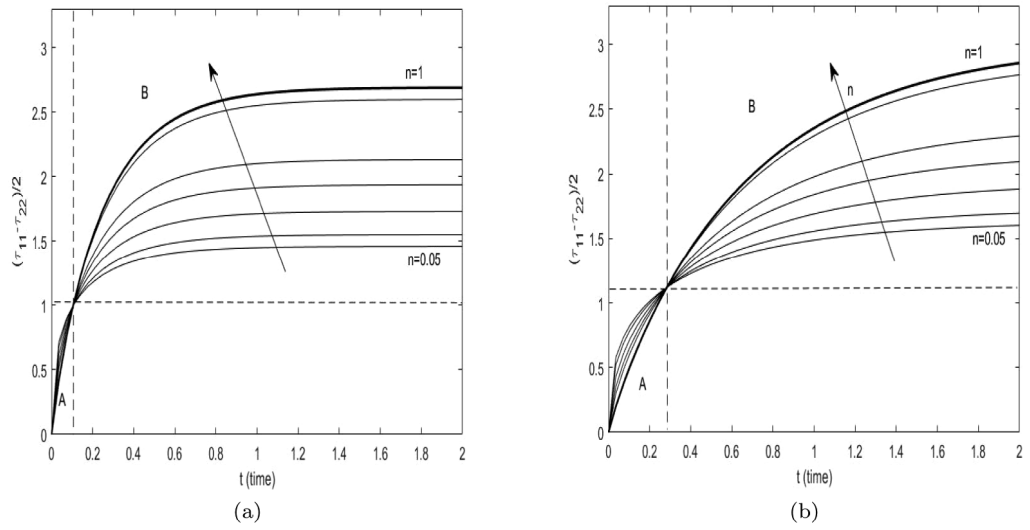

Fig. 3. Suitable zoomed-in versions of (a) Fig. 2(a) and (b) Fig. 2(b), respectively.

the origin does not represent the upper-bound solution (region A in Figure). However, compared to the previous case, the solution for n = 1 becomes an upper-bound solution when a longer time frame is used and also produces higher solution values. It can therefore be deduced that the case elaborated in this subsection is less consistent with the results obtained in [21], as the lack of fluctuations causes the solution obtained to be stable, unlike the instability shown in [21]. Finally, for $a = 0$, from the third equation in (70) we can easy see that $\psi = \frac{\Pi}{\zeta\dot{\gamma}}$, which represents the value of $\psi(t)$ when the regime condition is established.

7. Conclusions and perspectives

In this work, a search for correspondence between the theoretical mixture model for MR fluids solved in simple shear flow mode proposed by Chen & Yeh [16] and a experimental model of industrial interest proposed by D.S. Resiga [20] containing two components – Newtonian (elastic) & Herschel–Bulkley (plastic) – was conducted. Since, in the application field, the yield stress control determines the intended use of the product, we focused on the pre-yield region, limiting ourselves to considering only the plastic Herschel–Bulkley component (in pre-yielding, the elastic component is negligible) in the D.S. Resiga model. However, given the structures of both models, it was possible to verify the correspondence between by framing, on the one hand, the theoretical model in the EIT framework and, on the other hand, constructing the EVP generalization of the Herschel–Bulkley component of the experimental model in the GSM framework. Within these contexts, both models provided evolutionary constitutive equations, allowing a comparison to be conducted between them. Following a simplification of the Herschel–Bulkley EVP model due to the fact that in the operating conditions some terms can be considered negligible, the results showed good adherence of information content between the two approaches that, qualitatively, can be considered to be corresponding (at least in the chosen operating conditions). This allowed us to consider the EVP $3D$ component of Herschel–Bulkley to be an easily implementable alternative of the theoretical mixture model that presents prohibitive computational costs under the chosen operating conditions. Moreover, the numerical tests showed that the simplification implemented in the EVP model of Herschel–Bulkley produces a tolerable loss of information content. However, the qualitative analysis presented in this work is only a starting point for more in-depth research in which the quantitative aspect must be imperatively explored in order to differentiate the "bulk" component from the "shear" one, as the two are differentiated in detail in the theoretical mixture model. Finally, in the pre-yield region, the link $\tau_0 - \mathbf{B}$ must be specified in both models to connect $\mathbf{B}$ (and therefore the necessary electric current I in the coil) to guarantee the intended use of the product containing the MR material. In the near future, this link into account should be investigated to reformulate the

mixture model by introducing magnetic induction related to the fluid continuum so that, in the pre-yield region, the required link $\tau_0 - \mathbf{B}$ can be highlighted.

Acknowledgment

This work was supported by the Italian National Group of Mathematical Physics (GNFM-INdAM).

References

[1] I.A. Brigadnov, A. Dorfmann, Mathematical modeling of magnetorheological fluids, Contin. Mech. Thermodyn. 17 (2000) 29–42, http://dx.doi.org/10.1007/s00161-004-0185-1.
[2] R. Drouot, G. Napoli, G. Racineux, Continuum modelling of electrorheological fluids, Internat. J. Modern Phys. B (2001) 1–6.
[3] R.F. Harrington, Introduction to Electromagnetic Engineering, Dover Pubblications, Inc, Mineola, New York, 2003.
[4] K. Hutter, Van de Aaf Field Matter Interaction in Thermoelastic Solids, Springer-Verlag, New York, 1978.
[5] A. Hajalilou, S.A. Mazlan, H. Lavvafi, K. Shameli, Field Responsive Fluids as Smart Materials, Springer Nature, 2016.
[6] S.B. Choi, Y.M. Han, Magnetorheological Fluid Technology, Applications in Vehicle Systems, CRC Press, Taylor & Francis, Group Boca Raton, London, New York, 2013.
[7] P. Saramito, Complex Fluids, Modeling and Algorithms, Springer Nature, 2016.
[8] S. Khan, A. Suresh, N. SeethaRamaiah, Principles, characteristics and applications of magnetorheological fluid damper in flow and shear mode, Proc. Mater. Sci. (2014).
[9] W. Chooi, S. Oyadiji, Mathematical modeling, analysis, and design of magnetorheological (MR) dampers, J. Vib. Acoust. (2014).
[10] K.C. Chen, C.S. Yeh, Extended irreversible thermodynamics approach to magnetorheological fluids, J. Non-Equilib. Thermodyn. 26 (2001) 355–372.
[11] J. De Vincente, D. Klingenberg, R. Hidalgo-Alvarez, Magnetorheological fluids: a review, Soft Matter (2011).
[12] Y. Li, J. Li, W. Li, et al., A state-of-the-art review on magnetorheological elastomer devices, Smart Mater. Struct. (2014).
[13] Y. Nahmad-Molinari, et al., Sound in magnetorheological slurry, Phys. Rev. Lett. 82 (2001) 727–730.
[14] K. Ozsoy, M.R. Usal, A mathematical model for the magnetorheological materials and magneto rheological devices, Int. J. Eng. Sci. Technol. Elsevier 21 (2018) 1143–1151.
[15] D. Jou, et al., Extended Irreversible Thermodynamics, Springer, 2010.
[16] K.C. Chen, C.S. Yeh, A mixture model for magneto-rheological materials, Contin. Mech. Thermodyn. 15 (2002) 495–510.
[17] I. Cheddadi, P. Saramito, C. Raufast, P. Marmottant, F. Graner, Numerical modelling of foam Couette flows, Eur. Phys. J. E 27 (2) (2008) 123–133, No. 1.
[18] A. Farjoud, M. Ahmadian, N. Mahmodi, Nonlinear modeling and testing of magnetorheological fluids in low shear rate sueezing flows, Smart Mater. Struct. (2011).
[19] Y. Shen, M. Golnaraghi, G. Heppler, Experimental research and modeling of magnetorheological elastomers, J. Intell. Mater. Syst. Struct. (2004).
[20] D.S. Resiga, A rheological model for magneto-rheological fluids, J. Intell. Mater. Syst. Struct. 20 (2009) 1001–1010.
[21] P. Saramito, A new constitutive equation for elastoviscoplastic fluids flow, J. Non Newton. Fluid Mech. 145 (1) (2007) 1–14.
[22] E.H. Lee, Elastic-plastic deformation at finite strains, J. Appl. Mech. 1 (1969) 1–6.
[23] G.A. Maugin, The Thermomechanics of Plasticity and Fracture, Cambridge University Press, 1992.
[24] B. Halphen, Q.S. Nguyen, Sur les materiaux standard generalises, J. Mec. 14 (1975) 39–63.
[25] P. Saramito, A new elastoviscoplastic model based on the Herschel–Bulkley viscoplastic model, J. Non Newton. Fluid Mech. Elsevier 158 (1) (2009) 154–161.
[26] R.J. Gordon, W.R. Schowalter, Anisotropic fluid theory: a different approach tto the Dumbbell theory of diluite polimer solutions, Trans. Soc. Rheol. 16 (1972) 79–97.